University of Southern Queensland

Faculty of Health, Engineering and Sciences

Improved Transfer Chute Design Using DEM Software to Predict Material Flow Behaviour

A dissertation Submitted by

Alex Mason

in fulfilment of the requirements of

ENG4111 and 4112 Research Project

towards the degree of

Bachelor of Engineering (Honours) (Mechanical)

Submitted 25 August 2016

Abstract

Over the last decade the author has designed 20 or more chutes and been involved in the modification of 100's of others. However this work was all based on rules of thumb, with limited input from flow characteristics of the material being transferred. Although there are specific benefits to this rule of thumb based design, the end result is often a less then optimal chute design and the associated increase in operational costs.

The latest trend in chute design is to accurately model the granular flow through the chute using Discrete Element Method (DEM) software. The use of this software has been well documented in many research papers, particularly in the last 15 years. If used correctly DEM can serve as a valuable tool in predicting the behaviour of the granular material, highlighting the areas of impact and wear within the chute as well as the position, velocity and direction of the chute discharge, the latter of which is import in reducing belt wear of the conveyor.

The main objective of this project will be to investigate the use of Applied DEM's Bulk Flow Analyst software supplied by CABS Pty Ltd to analyse the flow in an existing transfer chute at Kwinana Bulk Terminal. This analysis will then be used to compare against an improved chute design in an attempt to improve the operation costs of the facility, specifically by the reduction down time, spillage and maintenance.

Disclaimer

University of Southern Queensland

Faculty of Health, Engineering and Surveying

ENG4111 & ENG4112 Research Project

Limitation of Use

The Council of the University of Southern Queensland, its Faculty of Health, Engineering and Sciences, and the staff of the University of Southern Queensland, do not accept any responsibility for the truth, accuracy or completeness of material contained within or associated with this dissertation.

Persons using all or any part of this material do so at their own risk, and not at the risk of the Council of the University of Southern Queensland, its Faculty of Health, Engineering and Sciences or the staff of the University of Southern Queensland.

This dissertation reports an educational exercise and has no purpose or validity beyond this exercise. The sole purpose of the course pair entitles "Research Project" is to contribute to the overall education within the student's chosen degree program. This document, the associated hardware, software, drawings, and any other material set out in the associated appendices should not be used for any other purpose: if they are so used, it is entirely at the risk of the user.

Certification

University of Southern Queensland

Faculty of Health, Engineering and Surveying

ENG4111 & ENG4112 Research Project

I certify that the ideas, designs and experimental work, results, analyses and conclusions set out in this dissertation are entirely my own effort, except where otherwise indicated and acknowledged.

I further certify that the work is original and has not been previously submitted for assessment in any other course or institution, except where specifically stated.

Acknowledgements

I would like to thank the project supervisor Dr Cahn-Dung Tran for his help and guidance on this research project.

I would like to thank Mark Rennie for his guidance, support and patience in helping complete this project. Mark assisted me in the choosing a suitable transfer chute for my project, facilitated the initial contact with Fremantle Ports and provided the resources required to carry the site visits and subsequent simulations. Mark also provided me a lot of invaluable information including the background of the port facility and suggestions in design improvements for this project, as well as financing a training course in the use of BFA software at Overland Conveyor office in Denver, Colorado.

I would also like to thank Fremantle Ports for allowing access to their facility in particular John Stewart for his interest and permission to conduct my project at Kwinana Bulk Terminal and Mufid Sain for his assistance with the site visits.

Finally I would like to thank my family for all the understanding and support rendered during the course of this research project.

Contents

Abstract ii

Disclaimer iii

Certification iv

Acknowledgements v

List of Figures ix

Appendices xvi

Glossary of Terms xvii

Chapter 1 Introduction 1

1.1 Introduction 1

1.2 Research Problem & Motivation 4

1.3 Research Objectives 5

1.4 Outline of research 5

Chapter 2 Background Research 7

2.1 Introduction 7

2.2 Literature review 9

2.3 Bulk Flow Analyst 26

Chapter 3 Simulation of the Chute Design 30

3.1 Introduction 30

3.2 Phase 1: Recording of transfer chute operation.. 31

3.3 Development of transfer chute design 34

3.4 Simulation of transfer chute using DEM 35

3.5 Resource requirements 44

3.6 Site Investigation 45

3.7 Site Visit 1 45

3.8 Site Visit 2 46

3.9 Site Visit 3 47

3.10 Conclusion 50

Chapter 4 CAD Modelling of Transfer Station 51

4.1 Introduction 51

4.2 Model Requirements and Rationalisation.. 51

4.3 Transfer Station Model 52

4.4 Conclusion 53

Chapter 5 Simulation of Existing Transfer Station 54

5.1 Introduction 54

5.2 Simulation Configuration 54

5.3 Material Parameters 63

5.4 Results 63
5.5 Conclusion 65
Chapter 6 Improved Transfer Chute Design 67
6.1 Introduction 67
6.2 Chute Modification Option 1 67
6.3 Chute Modification Option 2 69
6.4 Chute Modification Option 3 72
6.5 Conclusion 74
Chapter 7 Conclusion and Further Work 76
7.1 Achievement of Project Objectives 76
7.2 Conclusion 76
7.3 Further Work 78
References 80
Appendix A. 82
Project Specification 83
Appendix B. 84
Appendix C. 94
Appendix D. 97
Appendix E. 99

List of Figures

Figure 1-1 Shiploader dumping iron ore into the cargo hold of a bulk transport ship Source: www.fremantleports.com.au 2

Figure 1-2 Front end loader transferring iron ore from the stockpile to the loadout conveyor. Source: www.fremantleports.com.au 2

Figure 1-3 Stackers stacking iron ore in operation Source: www.fremantleports.com.au 3

Figure 1-4 Process flow diagram of Car Dumper Transfer Station. 4

Figure 2-1 Valley Angle Source: www.bulksolidsflow.com.au 11

Figure 2-2 Impact plate Source: David, S., 'Transfer Chute Design Fundamentals' 12

Figure 2-3 Rock Box Source: David, S., 'Transfer Chute Design Fundamentals' 13

Figure 2-4 Surge charge angle of belt conveyor Source: unknown 14

Figure 2-5 Preferred Arrangement of Load-out Chute Source: Arnold, P.C. 'Bulk Solids: Storage, Flow and Handling' 14

Figure 2-6 DEM simulation showing flow issues and improvement Source: Khambekar et al, 'Chutes and Suitability' 16

Figure 2-7 Belt misalignment due to off centre loading Source: www.shippbelting.com 17

Figure 2-8 Belt edge damage from misalignment Source: www.esseng.com.au 17

Figure 2-9 Relative Velocities of Lump to Belt Source: Arnold, P.C. 'Bulk Solids: Storage, Flow and Handling' 18

Figure 2-10 Angle of repose Source: Swinderman et al, ‘The Practical Resource for Cleaner, Safer, More Productive Dust and Material Control’ 20

Figure 2-11 - Shear Cell Source: (Swinderman et al. 2009) 21

Figure 2-12 - Mohr's Circle Source: (Swinderman et al. 2009) 21

Figure 2-13 - Internal Friction Angle Source: (Swinderman et al. 2009) 21

Figure 2-14 - Interface Friction Source: (Swinderman et al. 2009) 22

Figure 2-15 Particle overlap Source: (Favier et al. 2009) 25

Figure 2-16 Damped harmonic motion model Source: (Bharadwaj 2012) 25

Figure 3-1 Material Properties User Interface... 36

Figure 3-2 Boundary User Interface 38

Figure 3-3 Boundary with Traction User Interface 39

Figure 3-4 Extruded Boundary with Traction 40

Figure 3-5 Injection Box User Interface 41

Figure 3-6 Simulation User Interface... 42

Figure 3-7 100 x 100 mm grid on feeder side plate. 46

Figure 3-8 Vibration Stroke indicator on feeder 47

Figure 3-9 Time step sequence of particle past grid line. 48

Figure 3-10 Feeder bed depth 49

Figure 3-11 Read out from belt weigher. 49

Figure 4-1 Model of transfer station ... 53

Figure 4-2 Image of transfer station ... 53

Figure 5-1 Initial model overview ... 55

Figure 5-2 Injection box near side ... 55

Figure 5-3 Injection Box far side ... 55

Figure 5-4 Feeder near side ... 56

Figure 5-5 Feeder far side ... 56

Figure 5-6 Belt ... 57

Figure 5-7 Skirts ... 58

Figure 5-8 Feeder ... 58

Figure 5-9 Hopper ... 58

Figure 5-10 Hopper Height ... 58

Figure 5-11 Material build up and particle explosion. ... 59

Figure 5-12 Belt Friction Analysis ... 61

Figure 5-13 Mass Balancing ... 61

Figure 5-14 Good Material Spread ... 62

Figure 5-15 Marginal Material Spread ... 62

Figure 5-16 Poor Material Spread ... 62

Figure 5-17 Actual Material Spread ... 62

Figure 5-18 Basic and Delayed Configurations Bed Depth 63

Figure 5-19 Comparison of non-central loading 65

Figure 6-1 Insert Created in SolidWorks 68

Figure 6-2 Insert Positioned in BFA Model 68

Figure 6-3 Simulation of Option 1 69

Figure 6-4 Tapered Extension 70

Figure 6-5 Extension Positioned in BFA Model 70

Figure 6-6 Material Profile Comparison Showing Improved Load Centralization Profile View 71

Figure 6-7 Material Profile Comparison Showing Improved Load Centralization Top View 71

Figure 6-8 Insert Option 3, Vertical Sides with 80° Angled Back 72

Figure 6-9 Extension and Insert Positioned in BFA Model 72

Figure 6-10 Material Profile Comparison Showing Improved Material Profile 74

Figure B-1 Spillage adjacent to chute outlet. 85

Figure B-2 Longitudinal wear lines. 86

Figure B-3 Belt lift 87

Figure B-4 Flattening of belt at chute outlet. 87

Figure B-5 Tail pulley, left side. 88

Figure B-6 Tail pulley, right side 88

Figure B-7 View from tail end showing non- central loading on belt. 88

Figure B-8 One feeder in operation. 89

Figure B-9 Lack of load profile 89

Figure B-10 No back flow 89

Figure B-11 Backflow.. 89

Figure B-12 Surging.. 90

Figure B-13 Material slumping action 93

Figure C-1 Taken from Drawing 600196043-0100-ME-DRG-0001 95

Figure C-2 Taken from Drawing 600196043-0100-ME-DRG-0002 95

Figure C-3 Taken from Drawing K16350.. 96

List of Tables

Table 3-1 Resource Requirements ... 44

Table 5-1 Initial Injection Box parameters ... 55

Table 5-2 Initial feeder parameters ... 56

Table 5-3 Initial Conveyor parameters ... 57

Table 5-4 Initial Chute parameters ... 57

Table 5-5 Initial material parameters ... 58

Table 5-6 Initial simulation parameters ... 59

Table 5-7 Particle Size ... 60

Table E-1 Injection Boxes ... 100

Table E-2 Conveyor Belts ... 100

Table E-3 Feeders for Basic Configeration ... 101

Table E-4 Feeders for Delayed Configuration ... 101

Table E-5 Chutes ... 101

Table E-6 Material Radius 15 mm to 20 mm ... 102

Table E-7 Material radius 40 mm ... 102

Table E-8 Simulation Basic Configuration ... 103

Table E-9 Simulation Basic Results ... 103

Table E-10 Simulation Delay Start Configuration ... 104

Table E-11 Simulation Delay Start Results 105

Table E-12 Feeder Extensions 105

Table E-13Inserts 106

Table E-14 Simulation Configuration & Results for Insert Only 106

Table E-15 Simulation Configuration & Results for Feeder Extension Only....................... 107

Table E-16 Simulation Configuration & Results for Feeder Extension & Insert 107

Appendices

Appendix A – Project Specification

Appendix B – Record of Issues Found.

Appendix C – Drawings from FPA.

Appendix D – Equipment Measurements.

Appendix E – Simulation Results.

Glossary of Terms

The following abbreviations have been used:

3D	Three Dimensional
BFA	Bulk Flow Analyst
CAD	Computer Aided Drafting
CEMA	Conveyor Equipment Manufacturers Association.
CFD	Computational Fluid Dynamics
DEM	Discrete Element Modelling
FPA	Fremantle Port Authority
KBT	Kwinana Bulk Terminal

Adhesion	When material sticks to a surface.
Angle of Repose	The angle which the surface of a normal freely formed pile makes to the horizontal.
Angle of Surcharge	The angle to the horizontal which the surface of the material forms while at rest on a moving conveyor belt.
Belt	The rubber component that carries the material on a conveyor.
Belt Tracking	Axial movement along the pulley the belt makes during conveyor operation.
Beltweigher	An appliance that continuously weighs the conveyor belt to determine mass flow rates.
Bin	A large container that provides storage capacity for product.
Brownfield	Project that upgrades an existing plant or facility.
Bulk Density	It is the weight per unit volume of quantity of solid particles, expressed in kilograms per cubic meter.
Bulk Material	Granular material mass transported through a conveyor system. Also called material or product.

Car Dumper	A group of machines that systematically handles the removal of product from rail cars.
Carry	Top length of belt that carries the product from tail to head.
Carry-back	Material that has adhered to the belt and is carried back to the tail pulley.
Cohesion	When material particles stick to each other.
Dump	Discharge material from a height for storage.
Dust Extraction	Removal of dust laden air by suction nozzles and ducts.
Feeder	A machine the extracts a controlled flow of material from under a bin.
Fines	Material / particles smaller than 9.5mm in diameter.
Greenfield	Project that builds a brand new facility where no facility currently exists.
Head Pulley	Pulley at the discharge end of the conveyor. Belt goes from carry to return.
Hood	A product deflection plate that controls the trajectory of material as it discharges from the conveyor.
Hopper	The shaped conical section under a bin.
Impact Angle	Angle formed by flowing product and an internal surface of a chute.
Impact Plate	Plate used as a sacrificial surface for directing material flow, also known as bash plate.
Impact Zone	Area where the particles contact the receiving belt or equipment.
Inloading	Material coming into a facility.
Lining	Hard replaceable surface used for protection of chute structure.
Material	Used as an abbreviated form for bulk material.
Name Plate Capacity	The designed capacity of a processing facility. Usually in millions of tonestonnes per annum.
Outloading	Material leaving a facility.

Product	Granular material mass transported through a conveyor system. Also called bulk material or material.
Profile	The desired shape product forms on a conveyor belt.
Pulley	Cylinders which allow the belt to change direction.
Return	Bottom length of belt where the belt travels empty from head to tail.
Rock Box	The use of ledges to retain ore which in turn protects the chute structure.
Rotable Spares	Complete spare component designed for quick replacement.
Shiploader	Conveyor system designed for loading ships.
Spoon	A feed end deflector plate that is design to direct material in direction of conveyor.
Stacker	Conveyor system designed for dumping ore into stockpiles.
Stickiness	Slang - Cohesion.
Stockpiles	Large piles of ore stored prior to being processed or transported.
Tail Pulley	Pulley at the very back end of the conveyor. Belt goes from return to carry.
Transfer Chute	Structure that controls the flow of material from one piece of equipment to another.
Transfer Station	Structure that contains the transfer chute and all associated equipment.

Chapter 1 Introduction

This chapter will outline the intent of this project and the reason why it was chosen as a subject for this dissertation. Additionally it will provide an overview of the load facility at the Kwinana Bulk Terminal operated by Fremantle Port Authority.

1.1 Introduction

Fremantle Ports currently owns and operates the bulk material handling facility at Kwinana Bulk Terminal (KBT). In 2015 a total of 6.1 million tonnes of bulk material was exported through KBT of which approximately 4.5 million tonnes of that was iron ore (*Fremantle Ports Annual Report* 2015).

The majority of the land area in this port facility is utilised for stockpiles which are integral in facilitating rapid loading and unloading of the ships. While some stockpiles are located in large sheds for protection from the elements, the rest are stored in open areas known as stockpile yards.

Material to be exported from the port can be either trucked in by road or rail transport and is typically discharged or dumped into a hopper. Continuous transfer of the material from the hopper to the stockpiles and then from the stockpiles to the ship for export is carried out by a network of conveyors.

A brief description of each of the major steps in the conveyor network for iron ore is provided below, starting with the Loading/Unloading Jetty, then the Stockpile and finally the Car Dumper where material is brought in to the port from various mines.

1.1.1 Loading/Unloading Jetty

KBT loads and unloads a large variety of materials via its 498m jetty *Kwinana Bulk Berth 2*. A conveyor based transfer system known as a shiploader seen in Figure 1-1, is used dump the bulk material into the cargo hold of the ship. This method allows the material to move from a storage stockpile on land to the cargo hold as a continual process.

Figure 1-1 Shiploader dumping iron ore into the cargo hold of a bulk transport ship
Source: www.fremantleports.com.au

1.1.2 Storage Stockpile

There are a number storage stockpiles at KBT with iron ore, coal, mineral sands and bauxite bulk materials typically stored in the open air yards. Bulk materials are loaded from the stock piles onto the outloading conveyor via a number of front end loaders (Figure 1-2). This allows for a large amount of versatility in the selection of stockpile yard the bulk material is taken from, with a relatively low infrastructure investment.

Figure 1-2 Front end loader transferring iron ore from the stockpile to the loadout conveyor.
Source: www.fremantleports.com.au

The large open air stockpiles for bulk material at KBT are typically created by stackers, which operate in a similar fashion to shiploaders in that they utilise conveyors for the continuous transfer material as seen in Figure 1-3.

Figure 1-3 Stackers stacking iron ore in operation
Source: www.fremantleports.com.au

The benefit of having stockpiles in the facility is to allow better management of the ship loading operations. As the productivity of the Port is proportional by the number of ships it loads per year, there is a strong economic incentive in reducing the time it takes to load each ship. As such the stockpiles provide a buffer between the materials imported by rail and exported by ship. Additionally stockpiles allow the organisation of different materials produced from a variety of companies to be separately stockpiled.

1.1.3 Car Dumper

Finally the bulk material is fed to the stackers from the car dumper. The car dumper is designed to automatically empty trains loaded with material mined from various sites in WA. It works by sensing when an individual car is positioned correctly over the bin, then remotely opening the bottom of the car. The ore is then discharged onto 2 vibratory feeders via two hopper style outlets at the bottom of the bin. The vibratory feeders discharge onto the receiving RC01 conveyor (Fig. 4) through RC01 Feed chute.

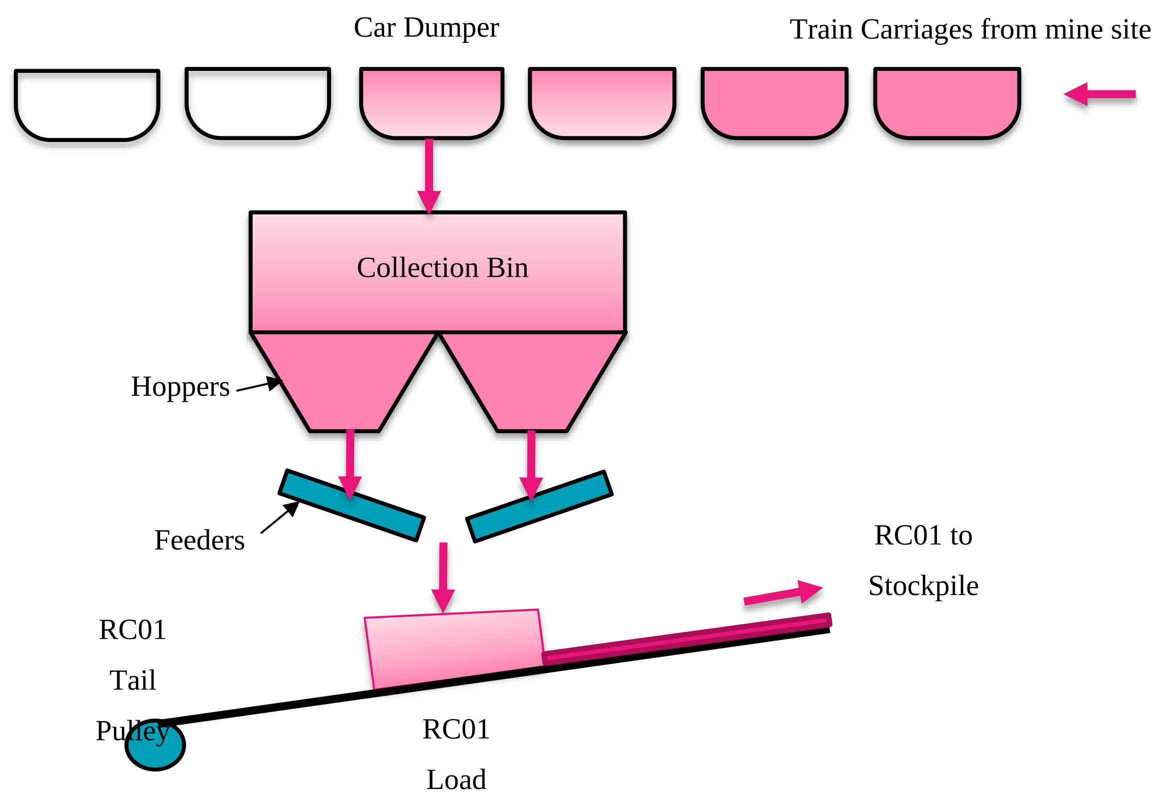

Figure 1-4 Process flow diagram of Car Dumper Transfer Station.

1.2 Research Problem & Motivation

An opportunity to improve the transfer chute at Fremantle Ports became available due to a proposed upgrade of the existing vibratory feeders under the car dumper bin. As there are some ongoing issues associated with this section of the material handling plant, an investigation into an improved design of RC01 Feed Chute and tail end of conveyor RC01 arrangement is proposed to try and address these issues. The benefit would be to use the major shut works required for the feeder change out to implement these solutions.

This project will use DEM modelling as well as conventional transfer chute design techniques to improve the transfer chute design such that significant benefit can be gained through reduce plant maintenance. The benefit of utilising DEM simulation in this situation is to adequately show improvements of the new design in comparison to the existing chute and thus provide confidence of success for any changes to the chute and hence reduce the risk of the project.

1.3 Research Objectives

The aim of this project is to improve the design of feed chute for RC01 conveyor, and then prove the benefits of the new design by using DEM simulation. The techniques developed in this project will be utilised on future transfer chute improvement projects.

The following tasks should be met to ensure the successful completion of this project:

- Conduct a literature review of transfer chute design and DEM modelling software.
- Define, record and model existing chute operation.
- Develop and use a systematic method used to adjust material properties in the model to accurately simulate real life chute operation.
- Optimise chute design to increase capacity and reduce spillage.
- Evaluate ore flow control under differing biased feed scenarios.

1.4 Outline of research

The research will present the use of DEM software and methods in transfer chute design. This dissertation is organised as follows.

Chapter 1 outlines the intent of this project and the reason why it was chosen as a subject for this dissertation. Additionally it will provide an overview of the load facility at the Kwinana Bulk Terminal operated by Fremantle Port Authority (FPA).

Chapter 2 provides the reader with a brief background of bulk material handling plants with a specific focus on transfer chute design methods, design decisions or design features which could result in poor performance of a chute. The chapter then finishes with a background in the development of DEM software and its use in bulk material handling industry. The use of this work will be the foundation of the improvements developed for the new chute design.

Chapter 3 will outline the methodology and techniques that will be utilised in firstly setting up the simulations, calibrating the model to recorded chute operation and analysing the results. It will also outline the findings of the three site visits conducted, detailing the issues found and measurements taken that will be used in the subsequent DEM analysis.

Chapter 4 will outline the creation of the CAD 3D model and its rationalisation for the use in the DEM software.

Chapter 5 will provide the set up and results from simulating the material flow through the existing transfer station set up in an attempt to replicate the issues noted in Appendix B. The simulation that best replicates the recorded flow issues will then be used in Chapter 6.

Chapter 6 will review the results of the existing and improved chute simulations and report on the comparative differences between the two designs.

Chapter 7 deals with the achievements, conclusions, recommendations and further work required to improve the transfer chute at Kwinana Bulk Terminal. It will also conclude this project.

Chapter 2 Background Research

This chapter will provide the reader with a brief background of bulk material handling plants with a specific focus on transfer chute design methods, design decisions or design features which could result in poor performance of a chute. The chapter then finishes with a background in the development of DEM software and its use in bulk material handling industry. The use of this work will be the foundation of the improvements developed for the new chute design.

2.1 Introduction

Conveyors are the prime transport method in bulk materials handling operations. Generally speaking, conveyors can only travel in straight lines, so transfer chutes are an essential element of a conveyor transfer system and cannot operate without them. Because successful operation of a transfer chute is essential for a conveyor system and non-performance of a conveyor system is extremely costly for bulk material operations, a lot of research has been conducted in the field of transfer chute design.

David Bickley (2011) states the following objectives of the transfer chute:

- To effectively control the transfer of the material.
- To minimise material degradation.
- To minimise dust generation and egress.
- To consider ease of maintenance e.g. rotatable spares.
- To minimise belt wear.
- To maximise the surcharge angle on the receiving conveyor.
- To effectively clean the belt, to minimise carry-back.

Historically or commonly, a transfer chute is designed to ensure material transferred from one conveyor or equipment to the other. Negating the other objectives, simple transfer chutes are relatively easy to design, particularly when dealing with dry, uniformly sized material. However, with each inclusion of the stated objectives comes an increase in design complexity due to the difficulty in accurately predicting material behaviour through the chute.

An example of the importance of material prediction occurs when looking at the chute discharge onto conveyors. With the correct design the ore stream can be controlled such that it is presented to the conveyor with the same velocity, thus reducing belt wear. As replacement costs of the conveyor belts can run into the $100,000's, not including the associated project and downtime costs that are inherent in a belt change out operation, accurately predicting the material behaviour at discharge becomes highly significant to the design process.

The reasons behind a simplified or poor transfer chute design developments are mainly economical, transfer chutes are generally designed to a level of accuracy that is implied in the engineering contract. This is particularly true in greenfield or new projects, where the focus of priorities are constructability, cost and safety. Colin Benjamin (2015) states in his book *The Transfer Chute Design Manual*;

"Time and money drives our industry so it is not surprising that something as banal as a transfer point in a conveyor system can be overlooked or poorly considered during any initial designing of a materials handling facility."(Benjamin et al. 2015, p. 7)

As a result some transfer chutes are designed based on general rules of thumb and designer experience (Hastie & Wypych 2010). These transfer chutes are generally designed based on historical designs of previous chutes or standard guidelines received from similar operations in the area. For greenfield sites, testing is often done on the ore to determine some material properties such as angle of repose and friction coefficient, and this information is used to help guide the designer in choosing which historical design will be best suited to the current situation.

Although, as stated earlier, there is significant benefits to investing in a good transfer chute design and this often does not occur for contractual / financial reasons, a macro-economic benefit can be seen for this situation. Process plants generally take time to reach name plate capacity and a poorly designed transfer chute may perform adequately at 50% -70% of name plate capacity. Here sound economic management is used to allow plant production to reach a point where a chute's poor design becomes an issue, during which considerable income will have been made with minimal adverse impact to the plant overall. At this point the plant operator may choose to invest in a new design to upgrade the existing chute and optimise the plant operation.

An existing chute upgrade will be primarily focused on chute performance. Here scale and computer modelling, in combination with data collected from the existing chute, can be used to great effect to improve an existing design. Additionally a significant cost benefit can be achieved if the improved chute design reduces plant bottlenecking or the downtime required to repair damaged equipment.

2.2 Literature review

A literature review was undertaken to further develop the idea towards a research project. The purpose of the review was to gather relevant information about:

- Review of Currently Design Methodology
- Issues from Poor Design
- What is Discrete Element Modelling
- Limitations of Discrete Element Modelling
- Calibrating Material Properties for Simulation
- BFA (Bulk Flow Analyst) Automatic Calibration

2.2.1 Review of Current Design Methodology

Historically a basic transfer chute design begins with identification of the material being transferred, the design flow rates and the feeding and receiving equipment. Minimum slope angles allowable for material to freely slide along the surface (1997) are determined and then from these angles a minimum height between feed in/out equipment can be found. At this point additional equipment such as belt scrapers, blocked chute switches and access hatches and so on should be considered. Finally installation support and maintenance considerations are included to complete a preliminary design.

A more detailed design will include some trajectory calculations based on projectile motion equations will give a rough estimate of material path through the transfer. Determining the trajectory allows the designer to implement some of the flow control methods such as; strategically positioned chute walls, rock boxes, bash plates and hood & spoon set ups. All of which have varying degrees of success at controlling the material flow according to the material properties.

This method is only successful when it is followed by a trial and error examination, either through physical modelling or onsite adjustments. Much research has gone into the accurate calculation of trajectory, particularly required when dealing with rock box based designs as well as hood and spoon type chutes. Here the accuracy of the materials trajectory path is needed to ensure it hits the right spot with the correct velocity vector.

Colin Benjamin (2015) wrote an excellent review on the main methods of current trajectory path calculations in chapter 3 of his book *The Transfer Design Manual*. He investigated the work by the following individuals and organisations:

- Method of Korzen
- Method of Booth
- Method of Golka
- Method of Dunlop
- Method of Goodyear
- Method of MHEA (Materials Handling Engineers Association) early and updated versions.
- Method of CEMA (Conveyor Equipment Manufacturers Association)

This work draws similar conclusions with Hastie's (2010) paper *The Profile of Conveyor Trajectories* and identifies that none of the mathematical models exactly represented the real life trajectory of the material, particularly when dealing with transient flow behaviour post impact within the chute. Additionally both Hastie and Benjamin identify scale modelling or investigation as the best method in deterring material trajectory and subsequent flow behaviour in new chute designs.

The simplest method of controlling material flow through the transfer chute is by allowing the material to slide down the internal surfaces of the chute. Use of strategically placed angled walls can control the direction and velocity of the material through the chute. Industry practice is to set the minimum internal wall angles at 70° to horizontal which is substantially greater than angle of repose plus 5º. Additionally the shallowest angle is the internal valley angle between two surfaces (Andrew L. Mular et al. 2002) (Figure 2-1). As stated earlier chute wall angles will drive the height requirement between the discharging and receiving equipment.

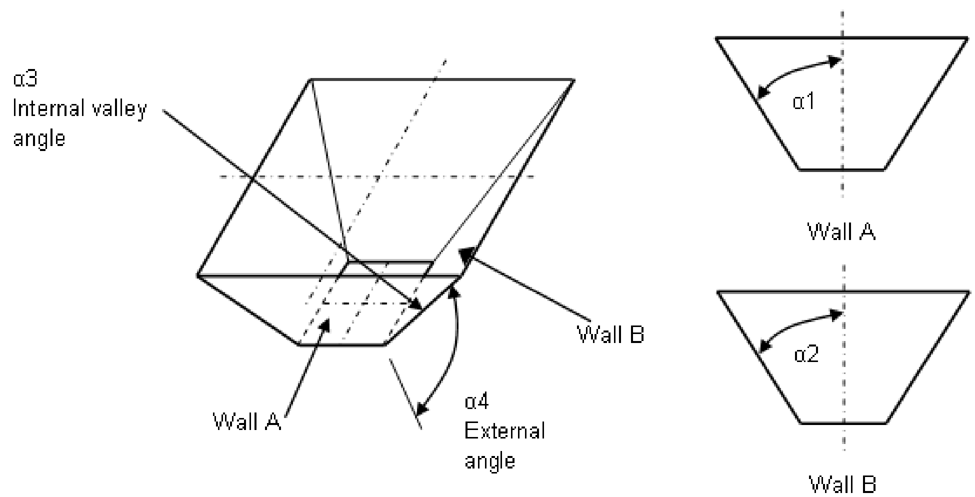

Figure 2-1 Valley Angle
Source: www.bulksolidsflow.com.au

The main drawback to this method is increased wear due to friction and if the chute wall angle is reduced too much then a capacity restriction can development leading to a chute blockage. Benjamin et al. (2015) states the chutes internal wall angle must be greater than the materials angle of repose and notes that other factors such as particle to wall friction, particle to particle friction, expected bed depth and the materials cohesiveness must be considered. This is similar to Arnold (1980) where he states that the chute angle should be 5° greater than the maximum friction angle between the material and chute wall to prevent capacity restrictions.

A slightly more complicated method of material flow control is by using impact plates such as the one shown in Figure 2-2. This is a crude method of controlling the direction of the material through the chute and is typically made of out of a plate lined with a harder steel tiles for wear protection Davis (n.d.). The main benefit of the impact plate is that it is adjustable allowing fine tuning of the materials trajectory during commissioning to ensure it lands centrally onto the receiving belt.

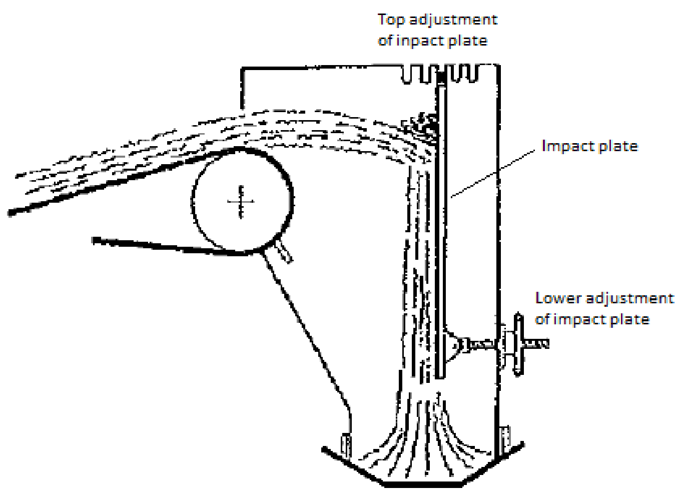

Figure 2-2 Impact plate
Source: David, S., 'Transfer Chute Design Fundamentals'

Rock boxes are cavities built into the chute wall typically at the impact point of the ores trajectory (Figure 2-3) primarily designed to handle the high impact and wear characteristics of falling material. During operation material is caught in the cavity and acts as a renewable wear surface for incoming material. Carefully placed, rock boxes in large chutes can effectively control the material flow by absorbing its kinetic energy reduce the particle velocity. If the height of the transfer chute is significant, then sequential rock boxes can be employed to create a cascading effect down the chute.

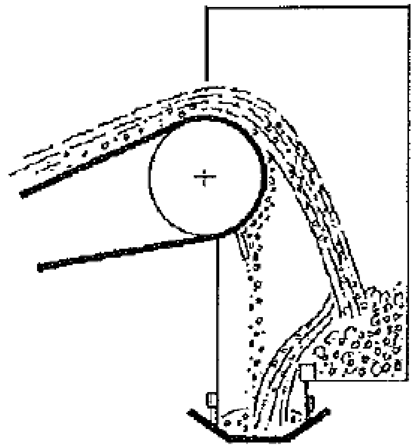

Figure 2-3 Rock Box
Source: David, S., ‘Transfer Chute Design Fundamentals’

There are, however, some associated issues with rock boxes that need to be carefully considered before employing them in a design (Benjamin et al. 2015):

- As their design inherently slows the material, a capacity restriction can develop in the chute.
- Additionally the reduction of the velocity normal to the conveyor direction is often associated in little or no outlet velocity in the belt direction. This will increase belt wear.
- The continual impact of ore on ore will increase the degradation of the material as well as dust and noise.
- They are prone to blocking when dealing with cohesive materials.

A good chute design will also allow for the development of the material profile on the receiving conveyor. The cross sectional profile of the material on the belt will ideally be the most stable shape that encompasses the largest area. Typically this shape, seen in Figure 2-4, is restricted by the edge distance, surcharge angle and conveyor belt.

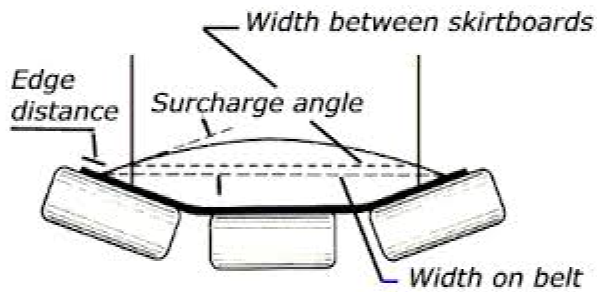

Figure 2-4 Surge charge angle of belt conveyor
Source: unknown

As the can be seen the majority of the material concentrated in the middle or flat section of the belt. P. C. Arnold (1980) describes a chute outlet design that facilitates the formation of desired profile shown in Figure 2-5.

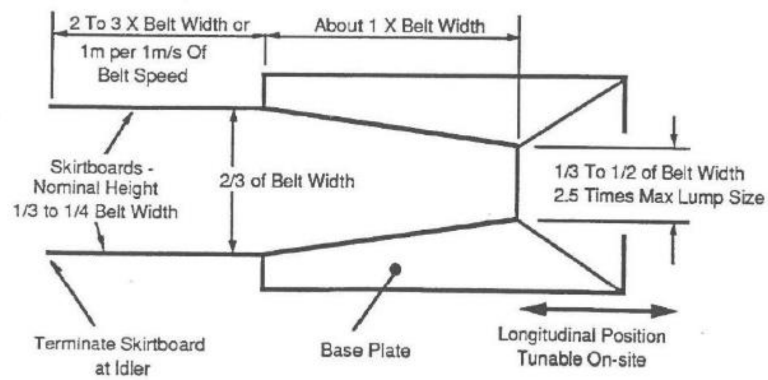

Figure 2-5 Preferred Arrangement of Load-out Chute
Source: Arnold, P.C. 'Bulk Solids: Storage, Flow and Handling'

The gold standard for flow control of material through a chute is the hood and spoon chute first conceptualised by Alan Huth in 1984 (Benjamin et al. 2015, p. 25). The basic premise of the design is to treat the material flowing through the transfer as a fluid and use a parabolic dish shaped hood deflector at the top of shoot and a similar shaped spoon deflector at the bottom. The hood is designed such that it receives the material from discharging belt and steers the material, firstly in a downward direction using the hood deflector then catching the vertically falling material and steering onto the belt with the same velocity vector as the belts using the spoon deflector.

There are many benefits to this type of chute design, including:

- Ability to handle cohesive and wet materials.
- Reduced dust generation.
- High capacity flow.
- Ease of maintenance.
- Use of rotatable spares.

Hood and spoon chutes are difficult and expensive design correctly as the angle of incidence on the hood, or angle of between free flowing material trajectory and the initial impact plate, is critical to the success of the design and must be as low as possible (Hastie & Wypych 2010). Additionally they are not overly well suited to highly abrasive materials. This can somewhat be alleviated through the use of high wear resistant liners with low coefficients of friction such as ceramics. Costing well over a $1000 per 300mm x 300mm tile, ceramic lining becomes an expensive perpetual maintenance cost.

2.2.2 Common Issues with Transfer Chutes

The design techniques identified in Section 2.2.1 are used to mitigate at variety of common issues found in transfer chutes. These issues include structural wear, spillage, belt wear, fire, capacity constraint and dust. Unfortunately the solution to one issue might cause the development of another. This section will investigate some of these issues and the design techniques available to resolve them.

As bulk material is typically abrasive, areas of structural wear develop at the contact points between the material flow stream and internal chute surfaces. As expected, this wear is proportional to the impact energy between the material and internal chute surfaces. The most common method to reduce structural wear is to line the internal surface with tiles made of a more wear resistant material known as liner plates and although they can be used by themselves, they are more effective when used in conjunction with other techniques which also reduce the impact energy of the material. One such technique is to reduce the angle of incidence between the internal surface and ore stream; techniques such as the hood and spoon are a good example of this. Slowing the ore flow through the use of chute geometry is another method in reducing impact energy, but must be balanced against the risk of flow restriction through the chute. The use of rock boxes at impact points is a highly effective and cheaper alternative to wear resistant liners for dry materials as it both absorbs the impact energy and slows the material flow through the chute.

Flow restrictions often occur due to insufficient incline of the chute surfaces and areas of stagnant flow and this is particularly prevalent in cohesive materials. As the material is slowed through friction along the chute sliding surface it will allow material to build up until it connects with the opposite side known as bridging. Figure 2-6 shows the DEM model of a coal transfer chute. As can be seen on the left hand image, material is slowing and building on the inclined surfaces, effectively blocking the chute (Khambekar et al. 2015). The right hand image shows how increasing the chute surface slope a significant reduction in build-up can be achieved. This effect can also occur with the use of rock boxes or deflector plates where incorrect placement can slow the material too much leading the material bridging. This issue is commonly known as choking and can be prevented with careful design.

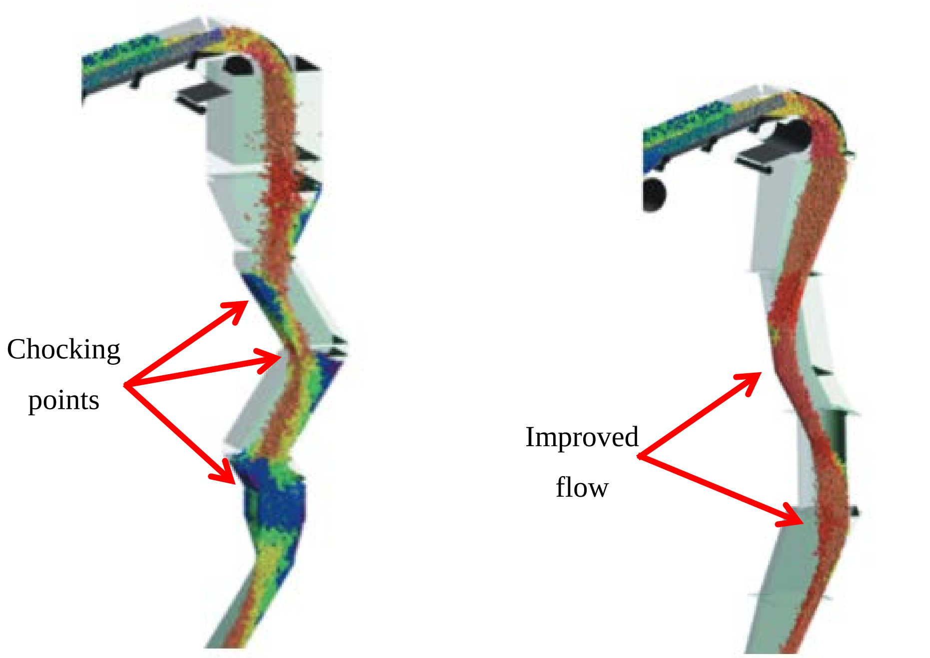

Figure 2-6a Poor design *Figure 2-6b Improved design*

Figure 2-6 DEM simulation showing flow issues and improvement
Source: Khambekar et al, 'Chutes and Suitability'

One of the fundamental requirements of the chute is that material must be loaded centrally on the belt (Benjamin et al. 2015; Davis n.d.). The use of inclined idlers on each side of the belt creates a trough and a non-centrally loaded material typically sits high up on of the side idlers as shown in Figure 2-7a. The material will re-centralise itself on the idlers through gravity and will drag the belt across the idlers as seen in Figure 2-7b. In addition to the excessive spillage, the edge of the belt will be prone to damage from rubbing against structures as seen in Figure 2-8 (CEMA 1997).

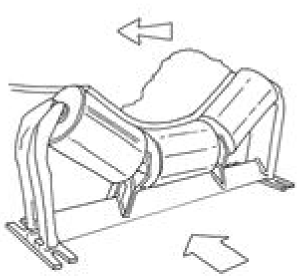

Figure 2-6a Belt loaded off centre

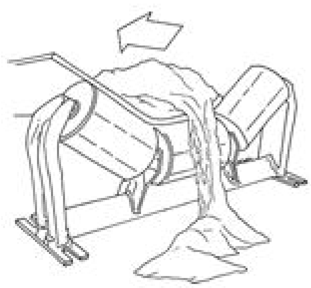

Figure 2-7b Material COG falling into trough of idler and associated spillage off edge of belt

Figure 2-7 Belt misalignment due to off centre loading
Source: www.shippbelting.com

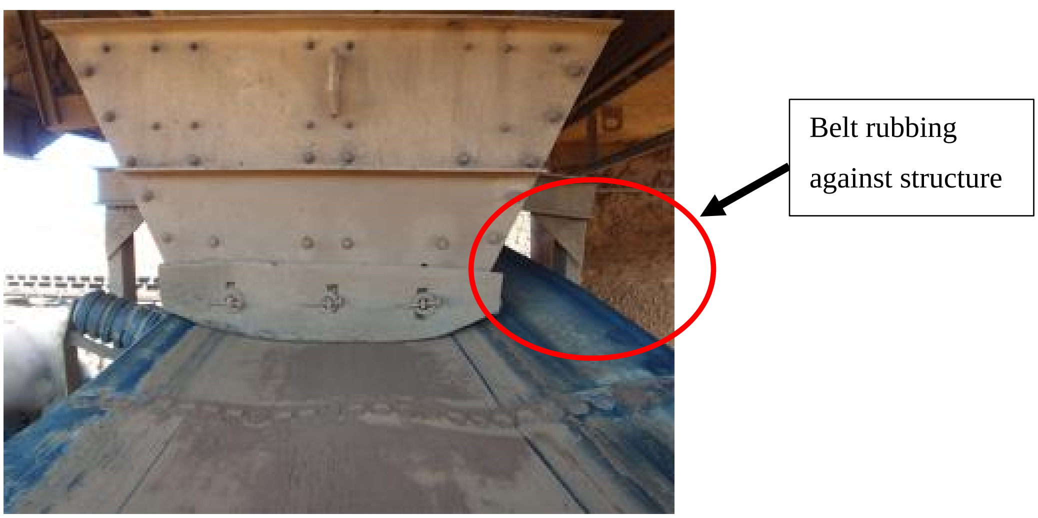

Figure 2-8 Belt edge damage from misalignment
Source: www.esseng.com.au

In addition to wear damage to the conveyor belt seen in in Figure 2-8, there is significant risk of fire as belts are manufactured from rubber. Fire can be initiated from the heat generated by friction between the conveyor belt and any stationary object such as the structure, a seized idler, perhaps build-up of spillage or carry back.

Another cause of spillage is through incorrect material profile development. If the material is not loaded with a suitable material profile as noted in Figure 2-4 and the belt is loaded to maximum capacity, then spillage is likely to occur at either the loading chute skirt outlet or at the next transfer - typically at the head end.

Poor flow control at the chute discharge will significantly increase the abrasive wear on the receiving conveyor belt. When material impacts the belt it causes abrasion, this abrasion is proportional to the impact pressure and the difference in velocity between the particle and the belt. If the material is not presented to the receiving belt correctly then an inclined angle of incidence will occur as seen in Figure 2-9. The resulting material inertia increases the friction between the material and belt causing belt wear. In severe cases the material may boil or roll on the belt becoming stationary reducing the flowrate out of the chute. As more material enters the chute, the mass builds up, proportionally increasing belt wear. By matching velocities significant improvements in belt life can be achieved.

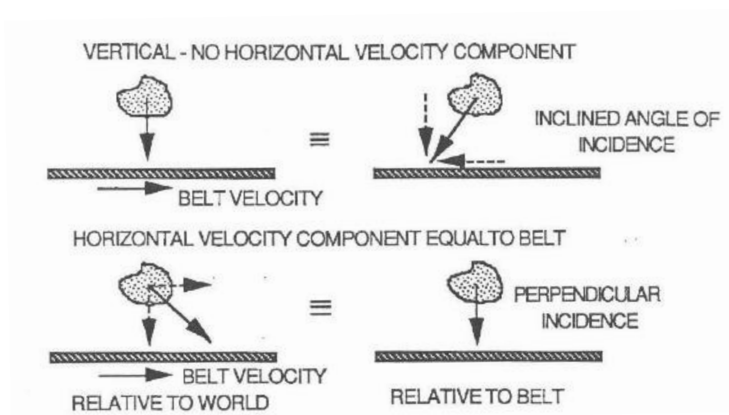

Figure 2-9 Relative Velocities of Lump to Belt
Source: Arnold, P.C. 'Bulk Solids: Storage, Flow and Handling'

One of the least desirable side effects of transfer stations, particularly with fine dry particles, is dust generation. Dust, along with noise, is one of the most common hazards for personnel working in transfer stations. At the extreme end, when handling organic material such as grains/flour, coal, wood products or fertilisers, the dust produced creates an explosive environment. Generally dust is considered a biological hazard due to issues associated with inhalation and skin/eye irritation. In addition to health and safety issues, consideration is given to product loss and degradation of associated equipment.

There are several products available in the market for controlling dust that attempt to seal the chute station and use extraction fans to create a negative pressure inside. These methods are expensive and requires additional infrastructure removing the dust from the extracted air. Additionally there is complex software for predicting dust generation using a combination of CFD and DEM software such as the open source software LIGGGHTS (Derakhshani et al. 2013).

However the simplest method is to use material flow control to prevent separation of the material as it falls through the chute. As the material flows off the conveyor, gradient of particles velocities develops based on the distance from the pulley centreline. The variation in particle speeds creates separation in the flow of the material and this separation draws and traps air in the material flow until it impacts on the belt. On impact the air is expelled from the material carrying the smaller lighter particles with it in the form of dust. By controlling the flow so that the stream remains as compact as possible, with minimal separation of the particles, dust generation can be significantly reduced.

2.2.3 Identifying Material Properties

Prediction of materials flow behaviour can be developed by identification of the various properties of that material. As such identifying these properties is an important part in determining a successful chute design. There are many methods for testing the various properties of bulk materials. Swinderman et al. (2009, pp. 399-402) lists 4 main properties that can be quickly identified;

- Bulk Density,
- Angle of Repose,
- Surcharge Angle and
- Material Size.

As mentioned earlier, the above properties are used in a basic or preliminary design of material handling equipment. Swinderman et al. (2009, pp. 402-6) also notes that improvements in material flow prediction can be achieved by additionally identifying the moisture content and internal shear limit of that material thus increasing the likely hood of a successful design.

Bulk density differs from particle density as it includes the air gaps between particles and can be further broken down by two measurements:

- Loose Bulk Density for design of areas where the material will be controlled in free flowing areas.
- Consolidated bulk density for design areas where the material becomes compacted through vibration or other means.

Typically we are concerned with loose bulk density when dealing with material flows.

The angle of repose is the natural angle a pile bulk material makes to the horizontal, refer Figure 2-10. While the surcharge angle is measured after a period of settling through vibration has occurred and used in determining cross sectional shape the material forms on a conveyor as seen in Figure 2-4.

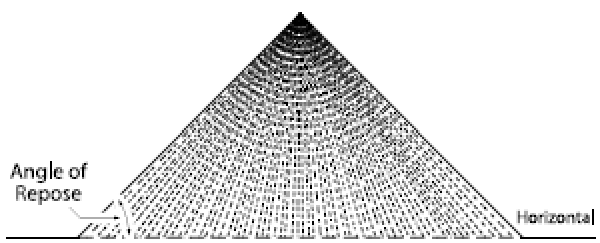

Figure 2-10 Angle of repose
Source: Swinderman et al, 'The Practical Resource for Cleaner, Safer, More Productive Dust and Material Control'

The material size is usually described as the width and height of the largest lump. For finer materials, particle size is determined by screening.

The internal shear limit is measured indirectly by determining the maximum force per unit area at which the material can resist separation from externally induced compression or sliding forces and is used to determine a materials internal friction coefficient. A typical shear cell shown in Figure 2-11, shows how the shear stress (S) and consolidated force (V) are determined. The shear and consolidated forces are used to determine flow ability of the material.

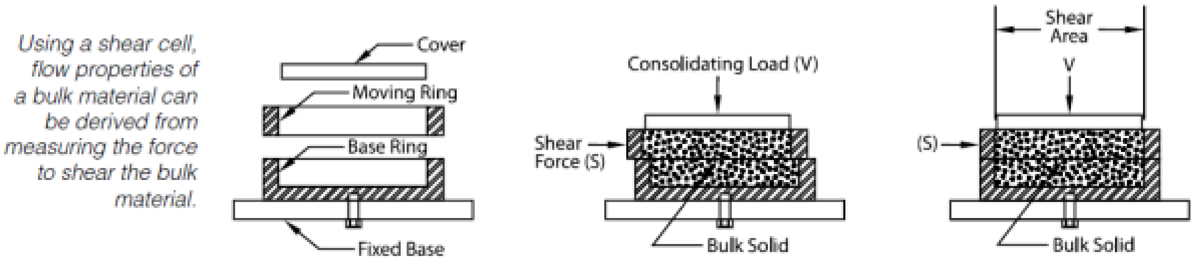

Figure 2-11 - Shear Cell
Source: (Swinderman et al. 2009)

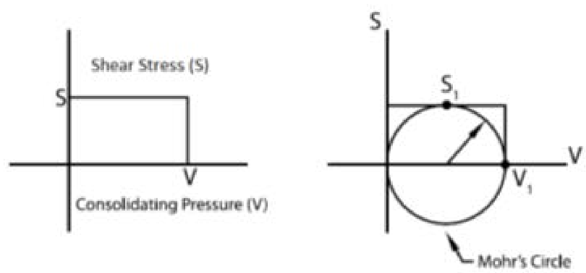

Figure 2-12 - Mohr's Circle
Source: (Swinderman et al. 2009)

As seen in Figure 2-12 a Mohr's Circle is developed and by increasing the consolidating pressure and recording the associated shear stress the internal friction coefficient can be determined, as seen in Figure 2-13.

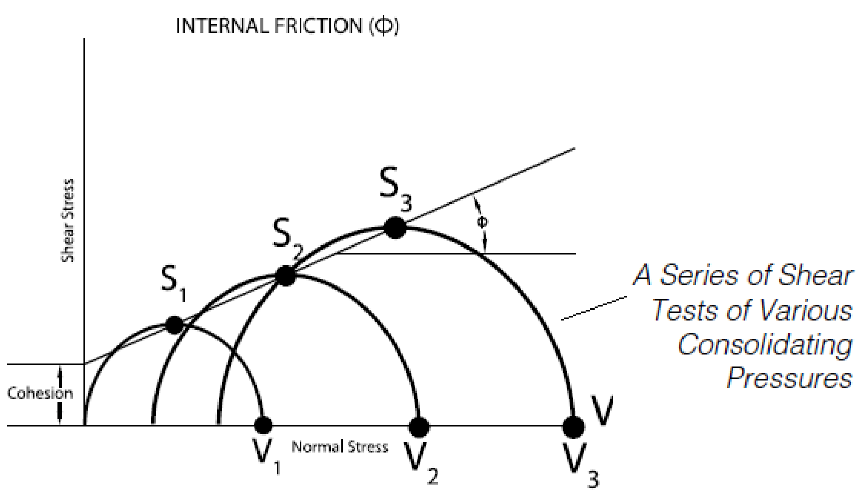

Figure 2-13 - Internal Friction Angle
Source: (Swinderman et al. 2009)

Similarly the interface friction (wall friction) is determined in a similar testing method, with the main difference being it is measuring the materials resistance to sliding over a surface rather than through internal shear as can be seen in Figure 2-14. Of note is the coefficient of friction (μ) is equal to the tangent of the interface friction angle (θ), and there is an inverse relationship between the consolidated pressure (V) and interface friction angle.

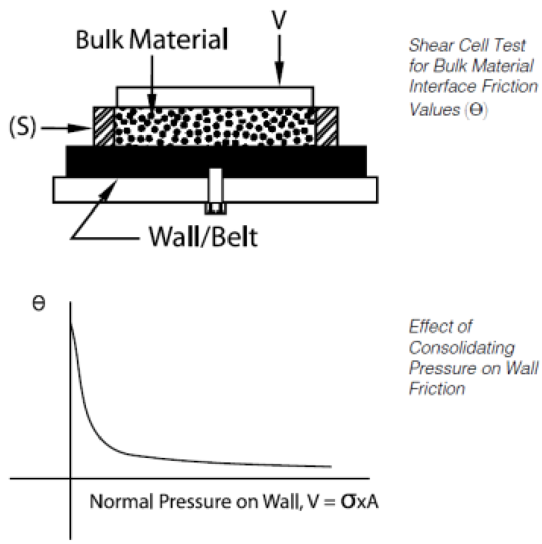

Figure 2-14 - Interface Friction
Source: (Swinderman et al. 2009)

Finally adhesion and cohesion are determined from the shear cell tests. Adhesion (σ) is the materials ability to resist movement at zero normal stress. Cohesion (τ) is the materials ability to resist shear at zero normal stress as seen in Figure 2-13. Cohesion and Adhesion are related to the interface friction angle, shear stress and consolidated pressure by the formula:

$$\tan\theta = \frac{S}{V} = \frac{\tau}{\sigma} = \mu \qquad (2)$$

Although the above information has been sourced exclusively from *Foundations – The Practical Resource for Cleaner, Safer, More Productive Dust & Material Control* (Swinderman et al. 2009) there was significant correlation with other literature including Schwedes and Schulze (1990) work on Measurement of flow properties of bulk solids, Bharadwaj (2012) and Grima et al. (2011).

Moisture content is the total amount of water in a bulk solid and is related to the cohesiveness and adhesiveness of a material. The moisture is measured as a percentage of the total wet weight of material. This is typically determined by drying the test sample to determine its dry weight as a comparison. It can be split into two types;

- Surface water – which is water that is free on surface, between particles and in open pores.
- Inherent water – which is water contained in closed pores, not including chemically bound water within particles.

2.2.4 What is Discrete Element Modelling

Discrete Element Modelling or DEM has been available for several decades and is a method used look at the interactions of a finite number of moving particles. This is achieved by modelling the associated contact and non-contact forces of particles (Grima et al. 2011). Grima further notes in his article that DEM can generate detailed particle flow trajectories and forces acting on individual particles as well as surfaces. This data can help gain valuable insight into the behaviour of bulk material flow through transfer stations as noted by Laurance Nordell (1997). Both papers highlight the significant benefits of utilising DEM to accurately model granular flow over other methods, not only as an improved chute design technique but also as cheaper method of verification of the design as compared with physical scale modelling.

It should however be noted that Grima's paper was sponsored by DEM Solutions Ltd, owner of proprietary software EDEM, and Nordell is the CEO of Conveyor Dynamics who specialise using Rocky DEM software to model bulk material transfer stations. Nordell's comments on Colin Benjamin's work *The Transfer Chute Design* in the Bulk-Online forum (Wöhlbier 2010) belay his preference to DEM software based solutions over traditional material trajectory and physical scale modelling based solutions.

DEM was first investigated by Peter Cundall (Cundall & Strack 1979) in an attempt to mathematically model inter-particle forces in granular flow in 1971. Although there were alternative mathematical modelling methods available at the time the DEM method was superior in the efficient use of memory space for handling the particle – particle interactions. He had qualitative success with his method when comparing to photoelastically obtained force vector plots produced by De Josselin, de Jong and Verruijt (cited in Cundall & Strack 1979). Although this method was based only on particles represented by two dimension disks in a plane. With the advent of improved computation power of the latest processors, this method has now been applied to not only three dimensional particles but also simulate particle material type and shape as with the EDEM software (DEM Solutions Limited 2016).

There are many papers and articles that outline how Newton's laws of motion form the foundation of DEM work, much of this literature is not surprisingly associated with proprietary software. As such the following explanation on the fundamental mathematics behind DEM modelling will utilise the extensive data base of articles provided by Janike & Johanson.

Bharadwaj (2012) describes the mathematics behind DEM software in his article. He notes that DEM is a mesh-free method that models individual particle forces. The boundaries of motion and geometry of surfaces is initially assigned by the user along with the particles to be analysed including starting position and initial velocities. Each particle is assigned a grid coordinate with the total forces acting each particle calculated, for each iteration of time, as the simulation progresses.

Both Bharadwaj and Grima note the particle calculations are based on the sum of mechanical contact and body forces:

$$F = F_{contact} + F_{body} = ma \tag{1}$$

Body forces are primarily gravity, however Bharadwaj notes cohesion, fluid drag and Van der Waals interactions can be included as body forces.

Contact forces are generally represented by damped harmonic oscillation as noted by Bharadwaj (2012), Grima et al. (2011) and Langston et al. (2004). Here the concept of particle overlap is used to describe the interaction when 2 particles collide. As can be seen in Figure 2-15 delta (δ) denotes the depth of overlap.

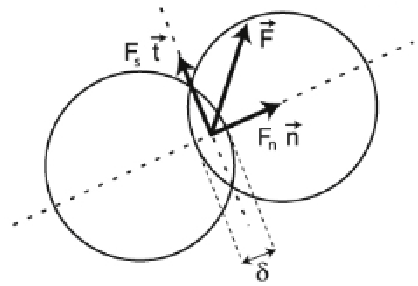

Figure 2-15 Particle overlap
Source: (Favier et al. 2009)

By using δ as the amount of overlap, its derivative δ' as impact velocity and combining in a damped harmonic motion model, natural phenomena such as material stickiness and Young's modulus can be represented. Figure 2-16 shows how the model can be set using the following formula;

$$F_{contact} = -K\delta - D\delta'$$

Where K is a function of the material size and stiffness developed from the material properties such as Young's modulus and D represent the coefficient of restitution or representing the material stickiness. This model also includes the friction coefficient μ representing surface roughness.

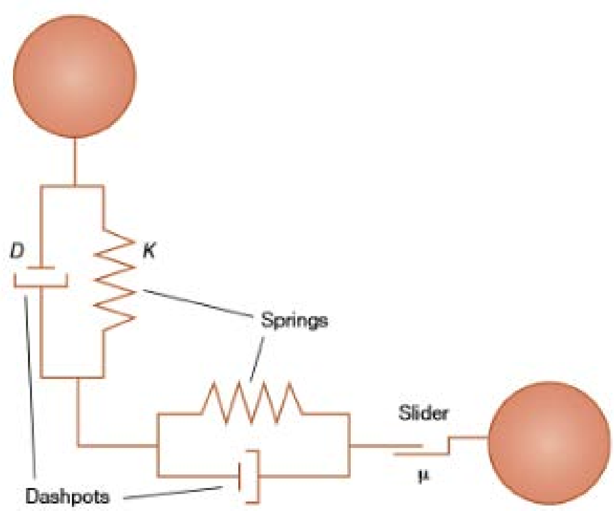

Figure 2-16 Damped harmonic motion model
Source: (Bharadwaj 2012)

2.2.5 Limitations of Discrete Element Modelling

Bharadwaj (2012) notes that there are still some considerable challenges in the use of DEM software and nominates the limitation in computational capacity as the primary challenge. As the method is designed to track every individual particles position, forces and velocity for each time step, increasing the number of particles increases the length of time taken for the computer to run the simulation. Additional complexities in the calculations also increase computational time. For example if the material has a high coefficient of restitution and or friction. Finally the particle shape can also significantly increase computation time compared to simple spheres, essentially the more realistic the model becomes the more computation time is required to run the simulation.

Bharadwaj also notes that model validation is another major challenge in the use of DEM software. Slight variations in composition of the material such as moisture and clay content affect the level of adhesive stress in materials (Swinderman et al. 2009, p. 406). If the model is not calibrated effectively to the material properties then there is a very high risk the model will not reflect actual material flow (Grima et al. 2011).

2.3 Bulk Flow Analyst

The following information was taken from Bulk Flow Analyst Workshop attended in February 2016, presented by Clint Hudson (2016), and covers some additional parameters not discussed in the literature review.

2.3.1 Automatic Calibration

An outline for setting up a material characteristic testing laboratory developed by Applied DEM is provided in Appendix A. By testing the material, a set of key parameters can be determined and inputted into the material calibration program. This program automatically calibrates the simulated material properties by using a grid method to choose the best results. Initially it runs four simulations based on random selection of four sets of key parameters with the selection range based on a grid. It then compares the results against the physically tested parameters and selects the closest match. The entire process is then run again but on a smaller selection range or grid of random parameters based on the difference between physical parameters and the chosen best fit parameters. This process is repeated until a desired level of error is achieved.

After some research and basic calculations of the feasibility of producing a simple yet basic laboratory, the author found that it would exceed the allocated budget and will substantially detract from the desired direction and intent of this report. Therefore material properties such as particle-particle friction and cohesion will be determined by trial and error while an industry average value of 1900 kg/m^3 and 2850 kg/m^3 will be used for the loose bulk density and particle density respectively.

2.3.2 Material size

Material size in conjunction with the density are important characteristics to be identified when trying to simulate flow through a transfer chute. Obviously an overly large particle will not accurately represent blockages in tight locations while smaller particles increase computational time. Material size is then a compromise between actual particle size, particle numbers and computational time. Minor changes in particle size can have significant impact in the calculation time required to run the simulation.

The comparative number of particles is inversely proportional to the radius ratio cubed as seen in the following equation.

$$N_S \approx N_L (\frac{r_S}{r_L})^3$$

Where N_S is the number of smaller particles required, N_L is the number of larger particles run and r_S & r_L are radius' of smaller and larger particles.

An estimate in potential increase or decrease in calculation time can be determined by ratio of radius to the fourth power as seen in the following equation.

$$\varphi \approx \left(\frac{N_P}{N_I}\right)^3$$

Where φ is the percentage change in calculation time, N_I is the number of particles run in initial simulation required, N_P is the number of proposed particles to be used in new simulation.

Adding variation in material size will prevent unrealistic behaviour in corners. This is due to a phenomenon where similar sized particles are more likely to stack up on themselves as they share similar centres of gravity. As such varying the size of particles induce instability in long stacks of particles. A variation in particle radius of 10% was advised as being sufficient compromise between inducing this instability and not significantly increasing simulation time.

2.3.3 Friction and Cohesion

The particles are spherical in shape to reduce calculation time, however real life particles are not uniformly round. This can be resolved by adjusting a combination of inter-particle friction and cohesion of the particle to particle contact. There set values available for initial simulations to provide a rough estimate for initial setups of material characteristics, such as the 5 options for Cohesive Condition; Dry , Slightly Sticky, Sticky and Very Sticky.

2.3.4 Surface entities

Surface entities are chosen from for specific reasons For instance, the outgoing conveyor will have a reduced coefficient of friction to highlight issues of poor chute design that could be hidden by the belt dragging the out the material rather than the chute shape controlling the flow in the correct direction. Additionally we are not concerned with issues with the feeder prior to entering the chute, so a high friction factor is required to ensure all material is transferred into the chute.

2.3.5 Time Step

"When DEM is used to analyse a particle system, each particle's position, velocity, forces and other information are known at given time increments called time steps."(Hudson 2016)

Time steps have a significant impact on the outcome of the simulation. Too small a time step increases the number of calculations required and hence the amount of time it takes to run the simulation. Too great a time step and there is a potential for the overlap distance during particle collision (δ distance in Figure 2-15) will be large enough that the resulting calculated rebound velocity is so high that the particles will behave in an explosive manner at the next time step.

The time step can be modified in BFA, however this can potentially create unrealistic representation of material flow. Alternatively a maximum velocity can be applied to the particles and the software will calculate a suitable time step such that no particle will surpass that velocity. Initially the maximum velocity is the free fall height of a particle through the total model height (height distance from particle generation to particle removal). Then after the first simulation the actual maximum particle velocity can be read from the results of the Particle Motion Analyst file and a resolved maximum velocity can be set at an arbitrary 10% above actual maximum particle velocity.

Chapter 3 Simulation of the Chute Design

This chapter will outline the methodology and techniques that will be utilised in firstly setting up the simulations, calibrating the model to recorded chute operation and analysing the results. It will also outline the findings of the three site visits conducted, detailing the issues found and measurements taken that will be used in the subsequent DEM analysis.

3.1 Introduction

The project is to be broken up into 4 phases:

Phase 1: Recording of chute

- Identification of potential chute, gathering the necessary resources and equipment to allow recording of existing material flow.

Phase 2: Modelling of chute

- Modelling the existing chute.
- Setting up and the calibrating the flow through the existing chute using DEM software
- Confirming the results of the calibrated flow against the recorded existing flow.

Phase 3: Analysis of data

- Analyse chute flow issues and determine appropriate solutions
- Design of modified chute to improve the material loading on outgoing belt.
- Re-run DEM model on improved chute design.

Phase 4: Presentation

- Development of written report for use in dissertation presentation.

3.2 Phase 1: Recording of transfer chute operation

The purpose of recording the transfer chute during operation is to initially create a base line or reference of the defects associated with the chute. This reference is then used to help develop solutions to the identified issues. The recordings final use after the completion of the project to compare against the improved transfer chutes operation, primarily as visual evidence of the resolved defects for the client. For this project I propose to also use this base line recording to calibrate a DEM simulation of the original transfer chutes operation and determine material flow of the feeders.

Additionally an approximation of the material flow rates will be calculated from a method of visually tracking a particle in the overall material flow. This will be done at 3 locations; mid-point of feeder bed, discharge from feeder and outlet of receiving conveyor. As the conveyor speed is known, the conveyor speed calculated from particle tracking will prove if the method is successful and provide an expected margin of error for speeds calculated for midpoint of the feeder bed and discharge point.

Additionally as there are various recording options available in the camera regarding frame per second rate and definition, the recordings for particle speed calculation will be done via the following settings.

- 4k resolution (3840x2160 pixels) @ 15fps.
- 1080p resolution (1920x1080) @ 60fps.
- WVGA resolution (848x480) @ 240fps.
- 2 sets of 12MPa stills taken at a burst rate 15 shots per second.

All other recordings will 1080p @ 60fps.

3.2.1 Equipment

The recording equipment we used needed to be capable of operating in a harsh environment and have the capability of relatively high definition images as well as high frame per second (fps) rate of recording. Additionally the recording device needs to be place in restricted access areas, so a requirement of being small, lightweight with readily accessible mounting accessories is desirable. As such a Go Pro Hero 4 Silver edition action camera was selected for the following reasons:

- Variable resolution and frame rates from 848x480 pixels @ 240fps to 3840x2160 pixels @ 15fps recording.
- 12 mega pixel still image.
- Simultaneous recording of video and still image.
- Availability of a large assortment of mounting components.
- Protective case for operating in harsh conditions.
- Light weight at 152g with protective case.

Finally the risk vs cost of the camera was the right balance. The next model up doubled the fps for high resolution recording, however was a 50% increase in cost, the significant increase in price made the risk of loss or damage too great to carry.

For access to restricted areas of the chute an extension pole was constructed with an attached lighting rig from an adjustable mop handle.

3.2.2 Method

The site visits will be split over three separate visits. The first for feasibility of access, investigation of issues associated with the transfer chute as well as identifying areas to place calibration markings for determining particle velocities. The second visit is to measure and draw calibration markings to determine particle movement and material bed depth. The third visit is to record particle movements relative to calibration markings on chute as well as any other recordings missed on first visit. Each visit will require a Pre-site and Post-work to ensure each visits success.

Pre-site

Pre site will involve all documentation and preparation required prior to access on site.

1. Obtain relevant permits and inductions to enter port operational facility.
2. Complete JHA for site inspection.
3. Check operability of equipment.

Post-Site

On return from site the recorded videos and stills will be catalogued. An estimate of the material flowrate will be calculated by tracking a particle across a number of frames in the recording.

1. Clean and return equipment.
2. Download data from SD card and catalogue.

Site Visit 1

Site visit will involve obtaining recordings of various positions on the transfer station. Each recording shall be of a minimum of 15 seconds in duration and the distance and position of the camera will be noted relative to a designated reference point.

1. Position camera such that it has view normal to the flow of material on the receiving conveyor, then record material flow on conveyor.
2. Position camera such that it has view normal to the flow of material on feeder bed, then record material flow on feeder bed.
3. Position camera such that it is normal to feeder discharge then record material discharge from feeder outlet.
4. Position camera such that it has a view of material **entering** chute looking from tail end of receiving conveyor. Record material entering the transfer chute.
5. Position camera such that it has a view of material **discharging** chute looking from tail end of receiving conveyor. Record material discharging from transfer chute.
6. Position camera such that it has a view of material **entering** chute looking from head end of receiving conveyor. Record material entering transfer chute.
7. Position camera such that it has a view of material **discharging** chute looking from head end of receiving conveyor. Record material discharging from transfer chute.
8. Record any other observed defects.

Site Visit 2

1. Prior to visit, review recordings of previous visit and identify suitable areas for recording.
2. Draw 100 x 100 mm grid lines, on feeder side plate, parallel to material flow in a suitable pattern to identify material bed depth. Individually number each line.
3. Measure dimensions A to S outlined in Appendix D.

Site Visit 3

1. Prior to visit, review recordings of previous visit and identify missing recordings.
2. Record feeder vibration amplitude.
3. Position camera such that it has view normal to the grid on feeder side plate and record material flow on feeder bed.
4. Obtain conveyor flow rate recordings from operator.
5. Record belt feeder velocity from beltweigher.

3.3 Development of transfer chute design

Here the intent is to produce a suitable model that can be imported into the BFA software for simulation. As the BFA software only uses surface geometries, only the inside geometries of the components need to be accurately modelled and any 3D CAD modelling software that can produce STEP files can be used to create the geometric surfaces. However if the design is successful, then the model will be used as the basis for the detailed design of the chute and as such consideration must be given for:

- Lifting requirements for construction and maintenance.
- Stiffening and support of the chute.
- Manufacturability of the component.
- Maximum component size for constructability and maintenance if area is restricted.

Hence it is important to not only design the geometry of the surfaces correctly, but the design must also consider the surrounding structure and equipment to ensure implementation of the design is possible.

3.3.1 Software Selection

BFA is capable of importing a STEP file which is a common file format for sharing 3D models between different CAD software, as such there was a choice of three software available for producing the required models; AutoCAD, Microstation and Solidworks. Each software is suitably capable of producing a suitable model with the only significant difference being that AutoCAD and Solidworks can be integrated with the BFA software. Additionally Solidworks is the only parametric based modelling software. Although AutoCAD and Microstation do have parametric capability, it is still based on a Boolean prismatic or "dumb" solid modelling. For this reason Solidworks was chosen as the modelling software.

Unlike Microstation and AutoCAD, Solidworks has two different file types for producing a complex computer model; the part file and the assembly file. Essentially an assembly file is made up of a number of components created in part files. The major benefit of this method is the potential to create easily modifiable parts that intelligently integrate with each other in the assembly file, however this can also be its major drawback. Careful planning must be taken when creating each part file to ensure that future modifications do not require a major redesign or a requirement of a new part to be commissioned.

3.4 Simulation of transfer chute using DEM

There are a number of parameters that need to be set to ensure that the simulation is a reflective of the actual chute operation. Conveyor Dynamics, who are the proprietary owners of the DEM software used for this project, have noted that some of these parameters are purposely skewed to look for specific issues in the transfer chute design. For instance, the purpose of the simulation is to determine the efficiency of the transfer chute and not the accurate representation of the feeder, and as such the feeder can be replaced by a conveyor with a high surface coefficient of friction. Similarly the outgoing conveyor will have a reduced coefficient of friction to highlight issues of poor flow in the chute design that could have been hidden by the belt dragging out the material. Essentially the skewed parameters help to readily identify a poorly performing chute design. An alternative method is to get the model to represent the real world as close as possible. A sensitivity analysis can be conducted once the model is calibrated.

The BFA software allows this control by building the model from a series of components. Each component is associated with a unique set of characteristics specific to that type of component. The following sections will identify each component type and give a brief explanation on the variable characteristics.

3.4.1 Material Properties

Material properties identify the specific characteristics of the material to be simulated. A table, shown in Figure 3-1 is used to specify density, size friction and stickiness properties.

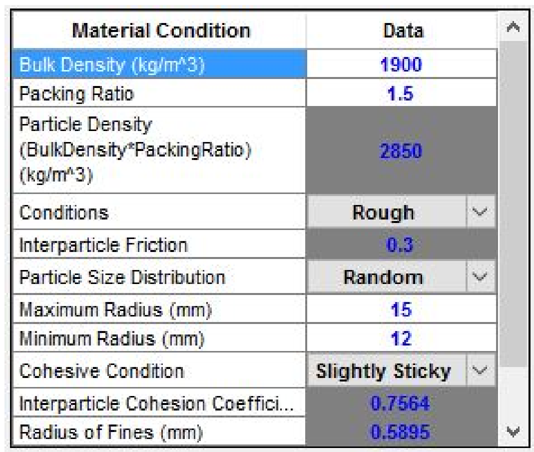

Material Condition	Data
Bulk Density (kg/m^3)	1900
Packing Ratio	1.5
Particle Density (BulkDensity*PackingRatio) (kg/m^3)	2850
Conditions	Rough
Interparticle Friction	0.3
Particle Size Distribution	Random
Maximum Radius (mm)	15
Minimum Radius (mm)	12
Cohesive Condition	Slightly Sticky
Interparticle Cohesion Coeffici...	0.7564
Radius of Fines (mm)	0.5895

Figure 3-1 Material Properties User Interface

The implication of varying these details is discussed in section 2.3. However the Bulk Density and Packing Ratio have been arbitrarily set at 1900 kg/m^3 and 1.5 respectively for all materials.

3.4.2 Surface Entities

There are three surface components will be created to represent the chute, conveyors and feeder associated with the transfer; Boundary, Boundary with Traction and Extruded Boundary with Traction. There are some common variables listed for each component type listed as follows

- **On Time and Off Time**

  Controls when the component is added and removed from the simulation.

- **Wall Friction**

Controls the surface friction coefficient between particles and the component surface.

- **Particle-Surface Adhesion**

  Controls the amount of coefficient of adhesion between the particle and the component surface. This is typically used for wet or highly cohesive materials and will be ignored for this inspection.

- **Stress Precision Index and Tessellation Tolerance**

  This is used for particle to surface impact investigations and will largely be ignored for this project.

The use of the following surface entities are detailed below.

Boundary is the simplest of the entities and is used to represent the non-moving surfaces such as chute walls and conveyor skirts. The variable to be modified in this instance will be the Wall Friction. Boundary Surfaces in this model will include the:

- Conveyor Skirts
- Feeder side plates
- Hopper
- Skirt Insert

Initially the coefficient of friction for the walls will be set at 0.5 to highlight accentuate areas of potential blockages. On subsequent simulations the friction will be reduced 0.3. These values where chosen arbitrarily to help identify the influence of wall friction has on the resulting material simulations. A rough guide to friction coefficients provided by the BFA (*Bulk Flow Analyst* 2016) software is as follows:

- Friction-less walls to smooth surfaces: 0 to 0.3
- Most dry materials: 0.3 to 0.6
- Rough rubber like surfaces: 0.6 to 2

Boundary	Data
On Time @__sec	-1
Off Time @__sec	5000
Wall Friction	0.5
Particle-Surface Adhesion	0
Stress Precision Index	1
Tessellation Tolerance	3.00
Moving Boundary?	None
Surface ID	s30
Comment	Prelim Geometry

Figure 3-2 Boundary User Interface

The variable 'Moving Boundary?' seen in Figure 3-3 can be used to simulate the action of a vibratory feeder by inducing a surface vibration. Components created in this project using Boundary entities will be labelled with the prefix 'Chute', while those with a vibration element to them will be labelled with the prefix 'Feedervib'.

This entity is similar to Boundary but has the added variable of a velocity vector used to simulate the surface motion parallel to the surface plan. Only the feeder components will be created using this entity and a coefficient of friction of 0.5 will be used for Wall Friction to reduce material flow issues prior to the discharge point of the feeder.

The surface velocity will be varied to maintain the mass balance flow rate between the material entering the feeder and discharging. An initial velocity will be determined using the following formula:

$$\frac{Q}{A} = v$$

Where:

- $Q =$ the volume flow rate.
- $A =$ is the cross sectional area of the feeder (Bed width x Bed depth)
- $v =$ is the resulting material velocity on the feeder.

The volume flow rate Q is related to mass flow rate $\dot{M}$ and the bulk density ρ_d by the folloing formula:

$$\frac{\dot{M}}{\rho_d} = Q$$

The bulk density has been set in section 3.4.1 as 1900 kg/m^3 and the mass flow rate is recorded from the site visits as outlined in section 0.

Boundary with Traction	Data
On Time @___(s)	-1
Off Time @___(s)	5000
Velocity (m/s)	0.27
Wall Friction	0.5
Particle-Surface Adhesion	0
Stress Precision Index	1
Tessellation Tolerance	3
Surface ID	s33
Comment	prelim geometry

Figure 3-3 Boundary with Traction User Interface

Components created in this project using Boundary with Traction entities will be labelled in the following form:

Feeder_XX_SYY

Where XX identifies which feeder it is NS for near side and FS for Far side based on standard conveyor profile convention. YY is the velocity Multiplied by 10. For example the near side component shown in Figure 3-4 will be:

Feeder_NS_S27

This final entity is similar to the Boundary with Traction entity with the addition variables of 'Segments' and 'Segment Length' and is used to simulate the conveyor component. The use of Segments allows a long conveyor surface to be created and still maintain suitable sensitivity for particle – surface impact analysis. For this project the segment x segment length was set at approximately 8 x 1000 mm with a stress precision index of 9. This allows a high degree of resolution for impact analysis on the conveyor surface. This impact analysis will help determine if the modified chute design will potentially reduce belt wear. Additionally the belt Velocity is to be set the belt velocity recorded as described in section 0.

Extruded Boundary with Traction	Data
On Time @___(s)	-1
Off Time @___(s)	5000
Velocity (m/s)	3
Wall Friction	0.32
Particle-Surface Adhesion	0
Number of Segments	8
Length per Segment (mm)	999.998
Stress Precision Index	9
Surface ID(s)	s17,..,s24
Comment	prelim geometry

Figure 3-4 Extruded Boundary with Traction

Components created in this project using Extruded Boundary with Traction entities will be labelled in the following form:

RC01_FrXX_SYY

Where XX is the friction coefficient multiplied by 100 and YY is the velocity Multiplied by 10. For example the component shown in Figure 3-4 will be:

RC01_Fr32_S30

3.4.3 Injection box

Injection boxes control the generation of the bulk material particles to be used in the simulation. Typically they are of a square shaped box with four sides and an opening at the bottom to allow the generated particles to fall through. Similar to Surface Entities detailed in the previous section, their existence in the simulation is controlled by On/Off Time variables

The three main variables modified for the different simulations are Injection Start, Injection Stop and Flow Rate. The amount of material generated or injected in the simulation is controlled by the 'Flow Rate' variable and is determined as previously outlined. Injection Start/Stop controls the length of time the injection box is generating particles.

Injection Box	Data
Default Material Ref.	Select Material
Injection Mode	Body Diagonal
On Time @___(s)	-1
Off Time @___(s)	5000
Injection Start @___sec	0
Injection Stop @___sec	20
Flow Rate (tonne/hr)	1300
Tessellation Tolerance	3.00
Surface ID	s2
Comment	

Figure 3-5 Injection Box User Interface

Components created in this project using Injection Box entities will be labelled in the following form:

Inj_XX_YYYY

Where XX identifies which Injection box it is NS for near side and FS for Far side based on standard conveyor profile convention. YYYY is the mass flow rate. For example the far side component shown in Figure 3-4 will be:

Inj_FS_1300

3.4.4 Simulation set up

Once all the necessary components have been created a simulation can now be set up. This is achieved by setting the frequency of each iterative step and how often data is recorded during the simulation and then identifying all of the components that will be present in the simulation. There is no limit to the number of components that can be selected however each component can only be selected once. When an Injection box is selected a material must also be selected.

The frequency of iteration is determined a combination of the 'Time Step' variable and 'Max. Speed'. Section 2.3.5 details the method to set the time step and max velocity. Similarly the 'Snapshot Frequency' and 'History & Force Output Frequency' outline how often data is recorded and also as a significant impact in simulation run time. A balance has to be made between the smoothness and accuracy of the recorded simulation and its expected run time.

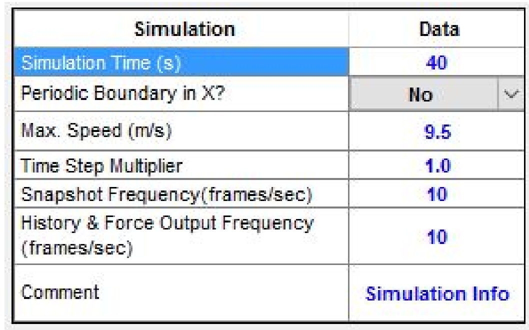

Simulation	Data
Simulation Time (s)	40
Periodic Boundary in X?	No
Max. Speed (m/s)	9.5
Time Step Multiplier	1.0
Snapshot Frequency(frames/sec)	10
History & Force Output Frequency (frames/sec)	10
Comment	Simulation Info

Figure 3-6 Simulation User Interface

Simulations created in this project will be labelled according to the following model set ups:

- **FP_Original_XX**

  Simulation based on existing transfer design.

- **FP_Original_Surge_XX**

  Simulations to replicate of surging.

- **FP_Orig_Insert_XX**

  Simulations of insert only.

- **FP_Orig_Ext_XX**

  Simulations of insert and feeder extension.

Where XX represents the sequential identification number of simulation.

3.4.5 Simulation Procedure

The following procedure was developed to simulate material flow through the transfer station:

1. **Identification of issues.**

   Not all issues can be replicated by the software, such as belt lift.

2. **Initial Model Build.**

   Identify the minimum values for each component

3. **Determine maximum velocity.**

   Section 2.3.5 details the method to set the time step and max velocity.

4. **Determine minimum particle size.**

   Minimum particle size is set by the 250,000 limit for total number of particles in simulation balanced against simulation run time.

5. **Test friction of belt.**

   Adjust belt friction so simulation matches real flow through impact zone.

6. **Run model for mass balance.**

   Adjust feeder speed to ensure full flow from injection boxes is transferred to RC01.

7. **Run first comparison simulation.**

   Run two simulations, first at larger particle size then at minimum particle size.

8. **Review identified issues against simulation results.**

   Compare model against recorded chute operation on the identified issues noted in step 1. Review feasibility of identified issues to be simulated and adjust as necessary.

9. **Adjust model parameters and Run comparison simulation.**

   Adjust model parameters as required to improve simulation comparison against actual transfer operation.

10. **Repeat steps 7 to 9 until suitable simulation of material flow is developed.**

It should be noted here that the DEM software can provide raw data of all the particles positions and velocities for each iterative time step, however the shear amount of data is difficult to visualize effectively through tables and or graphs. As such the software itself has built in graphic software to assimilate the data into an easily understandable visual representation in the form of a three dimensional animated simulation. A system of comparing the 3D still images of each simulation was developed to identify if the issues were effectively represented and which chutes were successful in resolving those issues.

3.5 Resource requirements

A resource analysis outlining equipment and software requirements for the project is provided in Table 3-1. CABS has agreed to provide in-kind access equipment, consumables and historical bulk material flow data. Phase 1 will require support from Fremantle Port Authority to provide the access to site for the chute inspection. Computer used for modelling and simulation work is supplied by the author and is not included in resource requirements.

Table 3-1 Resource Requirements

Item	Amount	Source	Cost
Measuring Equipment	One (1)	CABS	$10
Safety Equipment	One (1)	CABS	$200
Digital Camera	One (1)	CABS	$150
Digital Video Recorder	One (1)	CABS	$450
SD Card	One (1)	CABS	$25
Camera support brackets and light	Assorted	CABS	$80
Solidworks Design Package	One (1)	CABS	$4,000
Bulk Flow Analyst DEM software	One (1)	CABS	$15,000
		Total	$19,915

3.6 Site Investigation

Site visits were conducted for this project to identify the specific issues of the transfer station and record the data necessary to simulate the behaviour using DEM. The site visits were split into three individual visits with the methodology and requirements detailed in section 3.2 on page 31.

3.7 Site Visit 1

From the first site visit a number of issues were identified and a photo graphic record and is documented in Appendix A. These issues included:

- Spillage.
- Belt lift.
- Belt tracking.
- Non-central loading.
- Lack of material profile
- Some material back flow.
- Non-consistent feed rate or surging of material onto the receiving conveyor.

Some of these issues are interrelated and caused by poor flow control while others are related to the conveyor geometry. As this project is specifically looking at controlling the materials flow behaviour of the material, issues relating solely to conveyor geometry will be disregarded. As such the issue of belt lift will be ignored for this analysis.

The issues of non-central loading, belt tracking and spillage are interrelated as noted previously in section 2.2.2 with the root cause of these issues being non-central loading of the material on the conveyor. It also can be seen that there is no control of the material after it discharges from the feeders. This lack of control has contributed to the lack of material profile development and some of the back flow seen.

Additionally during the investigation the material appeared to hold together as it reached the end of the feeder until its weight would cause it to fracture at a point some distance from its discharge face. This resulted in the material performing a slumping action where large clumps of material would slide down the fracture face creating new discharge face at semiregular intervals. This effect is suspected to relate to the difference between shear strength under static and dynamic conditions once shearing has commenced, a similar effect can be seen in how avalanches are triggered. The downstream effect of this can be seen in the apparent surging of material on RC01 which will have a significant contributing effect to the issues of spillage and backflow. As such the identified issue of surging will need to be resolved to reduce the likelihood of spillage.

The identified issues of non-central loading, back flow and surging stated above can be remedied by controlling the flow of the material at the discharge point. It was speculated that chute insert placed between the feeder and RC01, which will centralize the material onto the belt in such a way that it allows the formation of a good material profile, the back of the insert will be sloped to allow some formation of velocity in the belt direction and the insert will have some capacity to hold the material allowing it to act as a buffer and reduce the surging effect.

3.8 Site Visit 2

After the issues were identified and a proposed solution developed a second site visit was conducted to perform measurements of existing transfer chute, as well as mark out gridlines to allow the measurement the current flow in the feeders.

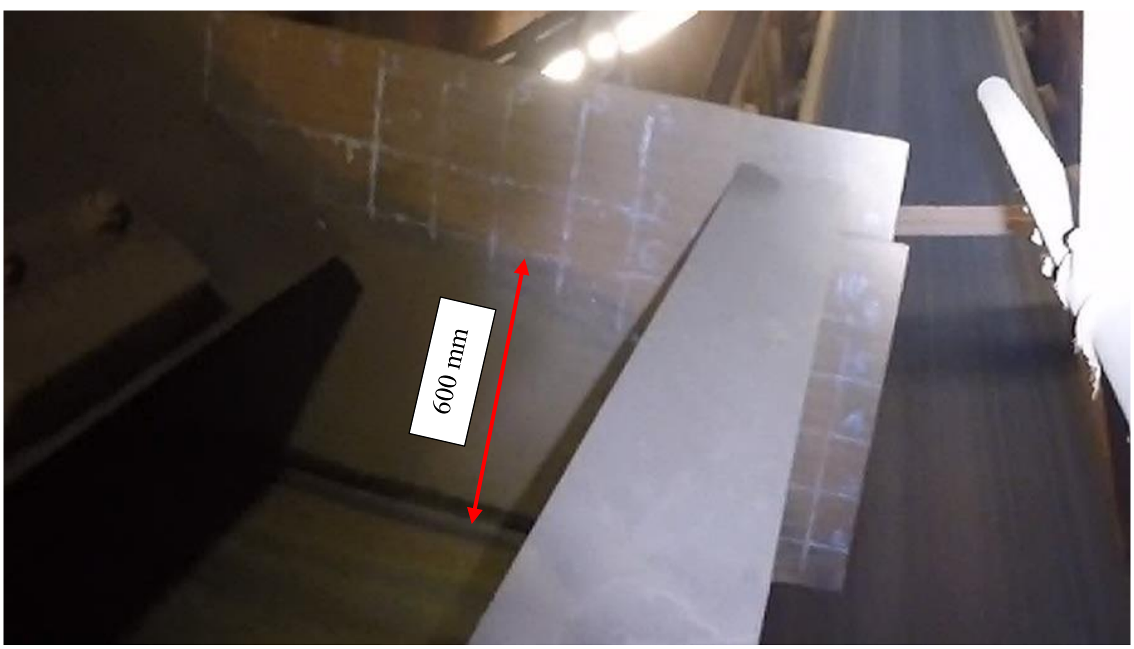

Figure 3-7 100 x 100 mm grid on feeder side plate.

Appendix C contains the existing drawings RC01 and its transfer chute, however due to a number of operational improvements that have occurred over the years, onsite measurement of the chute were critical to ensure that the drawings were accurate and all modifications were accounted for. During this visit measurements were taken to check the drawings accuracy and are shown in Appendix D. Figure 3-7 shows the grid drawn on the feeder side plate, for clarity the 600 mm height line from feeder bed is marked on the image.

3.9 Site Visit 3

The final site visit allowed the recording of key material flow rates seen on the feeders and conveyor as well as measuring bed depth.

3.9.1 Vibration Amplitude

Figure 3-8 Vibration Stroke indicator on feeder

The amplitude of the feeder vibration can be read from the indicator in Figure 3-8 as approximately 1.6 mm. Investigation of the similar machines from Syntechtron show a frequency of 50 Hz.

3.9.2 Feeder Flow Rate

(a) Frame 0 - Time 0.00 s

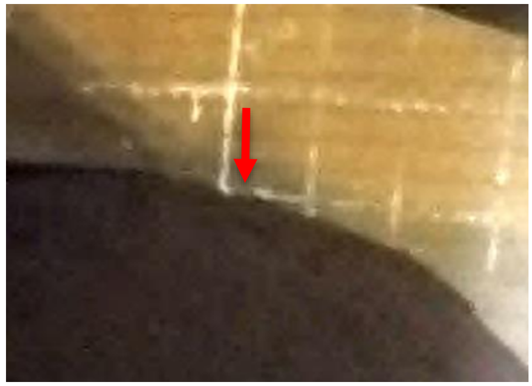

(b) Frame 15 - Time 0.125 s

(c) Frame 30 - Time 0.25 s

(d) Frame 45 - Time 0.375 s

(e) Frame 60 - Time 0.50

Figure 3-9 Time step sequence of particle past grid line.

A particle, identified by the red arrow in Figure 3-9 (a) to (e), is tracked as it travelled passed the grid lines marked out on the feeder side plate. The frame frequency of the recording was 120 fps and the particle took 60 frames or 0.5 seconds travel across a single grid, resulting in an approximate speed of 0.2 m/s.

3.9.3 Feeder Bed Depth

Figure 3-10 Feeder bed depth

Figure 3-10 Shows the bed depth of material on the feeder as being approximately 600 mm.

3.9.4 Conveyor Speed

RC01 Conveyor speed was taken from the beltweigher at 2.16 m/s as seen in Figure 3-11.

Figure 3-11 Read out from belt weigher.

3.10 Conclusion

The three site trips were successful in getting the required data to create the 3 dimensional CAD model and for initial parameter settings for simulation. The first visit was to identify issues that are to be resolved within the transfer station and the next two were to collect specific data to facilitate the development of the DEM simulation.

There were a number of issues identified during the first site visit as shown in Appendix A with many of those issues are interrelated and or systems of other design flaws. Some issues are not able to be simulated by the DEM software supplied such as those related to conveyor geometry and as such the issues chosen to be resolved include;

- Non-central loading
- Back flow
- Surging

The second and third site visit were primarily focused on recording data for building the models for simulation. Although this was overall successful, there were some issues with quality of the data that are noted as follows:

- The vibratory feeder is suspected of having a variable amplitude and frequency. A request for confirmation of this has been sent to FPA and at the time of writing this report no response has been received.
- Contrary to the method outlined, the recording to be used for determining particle velocity and bed depth of the feeder was not taken normal to the feeder side plate.
- The conveyor has a 91 m concave bend at the load point causing the belt lift at the idlers. Where on site measurements taken from top of belt, an attempt was made to push the belt down onto idlers by body weight. Success of this method could not be confirmed on site.
- The opening height of the hoppers to the feeder bed (dimension C in Appendix D) was not taken as to reach that point in the chute a confined space isolation was required necessitating a complete wash-down of the bin and hoppers. Due to financial and time restrictions this could not be achieved for site visit 2.
- The belt transition was also not measured, as such the idler angle dimension R in Appendix D was taken from the carry idlers at the skirting outlet.

Chapter 4 CAD Modelling of Transfer Station

This chapter will outline the creation of the CAD 3D model and its rationalisation for the use in the DEM software.

4.1 Introduction

From the previous site investigation a rationalisation of the data is required to produce a suitable CAD model of the transfer station to be used in by the DEM software. The following section will identify the model requirements and rationalisation of the data then finally detailing the resulting model.

4.2 Model Requirements and Rationalisation

4.2.1 Stiffeners and Supports

There were several elements that where omitted in the modelling process to reduce production time. The most significant was all components and structure on the outside the material contact surface. This includes everything below the top surface of the conveyor belt, all stiffening and support structures of the skirting, motor and structural supports of the feeder and so on. For the simulations to replicate the original transfer chute set up this had no impact on the outcome. However care should be taken when modelling the chute modifications to allow enough room behind the material contact surface for plate thickness, stiffening and supports.

4.2.2 Conveyor Concavity

The existing conveyor has a 91m concave radius at the point of discharge. This has been highlighted as a contributing factor to the belt lift issued noted in Figure B-3 in Appendix A. Due to the difficulty in converting the concave belt surface into a usable element in BFA an belt incline angle of 10° was chosen as this was the angle measured between the loading zone and skirting outlet. Similarly an analysis by AECOMM has been previously conducted with their recommendation of lowering the tail pulley to remove the concavity of the belt. This will create a straight section of belt though the loading area at an angle of incline of 10°.

4.2.3 Belt Transition

The loading zone of RC01 also occurs at the end of the transition zone of the belt. The transition zone is the section of belt where it converts from having a flat profile on the tail pulley to a troughed profile for carrying material along the conveyor. An attempt was made to measure the transition through the variation in the trough angle of the idlers over the loading area, however an incorrectly recorded measurement, plus unexpected variations in other measurements caused significant doubt over the accuracy of this data. As such an average trough angle of 15° was chosen for the entire length of the loading zone. The effect of this will likely cause the material to centralise better on the belt during DEM simulations.

4.2.4 Hopper, Bin and Feeder Length

As the model is primarily concerned with the outlet of the feeder onto RC01 conveyor belt, the hopper to feeder transfer was model in such a way that it allowed the material bed depth to be varied. Again to reduce production time an estimate was made of bin size such that sufficient delivery of material at required flow rate and bed depth could be maintained.

4.3 Transfer Station Model

Figure 4-1 shows the final model produced using Solidworks. The model is made up of 7 individual part models and then assembled in a single separate model. As can be seen from Figure 4-2 and Figure C-3 in Appendix C, there is a difference between the model created for simulation and the existing chute. The most notable difference is the large injection boxes used for DEM simulations that will be detailed in the next chapter.

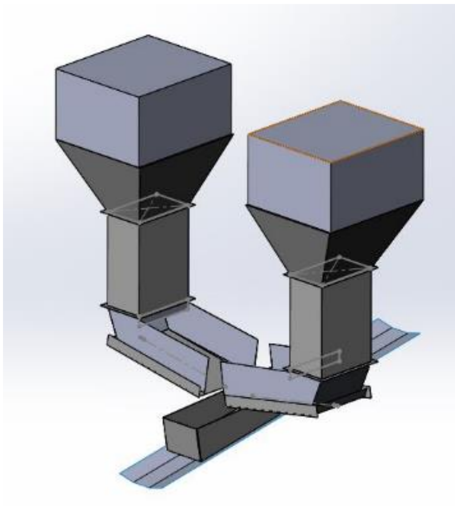

Figure 4-1 Model of transfer station

Figure 4-2 Image of transfer station

4.4 Conclusion

Solidworks was chosen as the preferred software due to its parametric modelling capability and availability of software integration support through Overland Conveyor Inc. However BFA's ability to accept STEP files allows the model to be created with any software that can produce a 3D model.

The data that was collected during the site visits was rationalised to allow for errors made during recording and to reduce to complexity of the model, as such the belt transition, belt concave curvature and feeder length are not an exact replication to the existing transfer station. Although there is variation, the results of the simulation are not expected to be significantly impacted given this is a comparative analysis.

Chapter 5 Simulation of Existing Transfer Station

This chapter will provide the set up and results from simulating the material flow through the existing transfer station set up in an attempt to replicate the issues noted in Appendix B. The simulation that best replicates the recorded flow issues will then be used in Chapter 6.

5.1 Introduction

Section 3.4 outlines the methods for establishing the base parameters for each component and the simulation procedure for the BFA software. The following sections will provide the results of this analysis organised in the procedure as outlined in section 3.4.5, followed by a summary of the results.

5.2 Simulation Configuration

The Simulation Procedure outlined in section 3.4.5 will provide the structure for the detailing the following results. Appendix E contains tables detailing the parameters for each component and tables detailing the parameters, components and results of each simulation run.

The Simulations where run using a MSI WT72 20M-1024AU laptop which contains a 4 core i7 4720MQ processor hyperthreaded to simulate 8 cores, 16GB of RAM and static hard drive.

5.2.1 Identification of Issues.

As stated in the section 3.10 the following issues were identified as being potentially simulated by DEM.

- Non-central Loading
- Back Flow
- Surging

5.2.2 Initial Model Build

The following parameters were identified as for the initial model setup and are listed by component. Figure 5-1 shows this initial model imported to BFA from Solidworks.

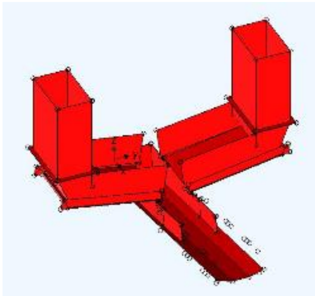

Figure 5-1 Initial model overview

Injection Box

The flow rate was identified as approximately 2200 tonnes per hour as per Figure 3-11.

Table 5-1 Initial Injection Box parameters

Component Name	**Inj_FS/NS_1300**
Time on (s)	-1
Time off (s)	5000
Inj Start (s)	0/3
Inj Stop (s)	20/20
Flow Rate (t/hr)	1300*
Tessellation Tolerance	3

* Estimate only as initial simulation was run between site visit 2 and 3.

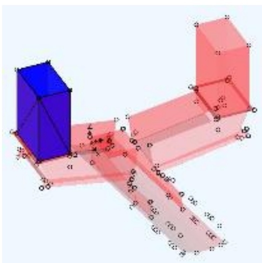

Figure 5-2 Injection box near side

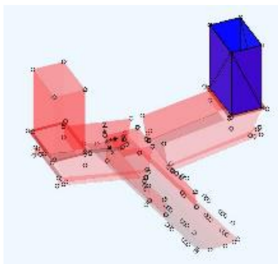

Figure 5-3 Injection Box far side

Feeder

Initial feeder settings were identified as a bed depth of 600 mm and material flow velocity of approximately 0.2 m/s as noted in Figure 3-9 and Figure 3-10.

Table 5-2 Initial feeder parameters

Component Name	**Feeder_FS/NS_S27**
Time on (s)	-1
Time off (s)	5000
Velocity (m/s)	0.27*
Wall Friction	0.5
Particle Surface Adhesion	0
Stress Precission Index	1
Tessellation Tolerance	3

* Estimate only as initial simulation was run between site visit 2 and 3.

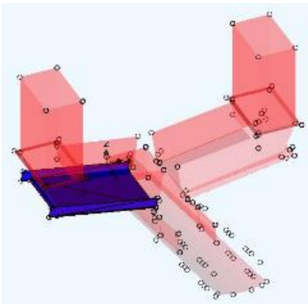

Figure 5-4 Feeder near side

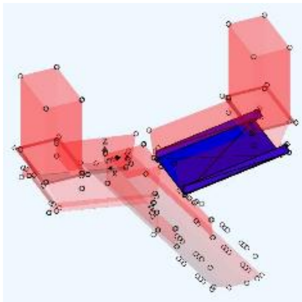

Figure 5-5 Feeder far side

Conveyor

Belt speed was identified at 2.16 m/s as per Figure 3-11 and the coefficient of friction was set 0.32 as per the discussion in section 2.3.4.

Table 5-3 Initial Conveyor parameters

Component Name	**RC01_Fr0-32_S3-0**
Time on (s)	-1
Time off (s)	5000
Velocity (m/s)	3*
Wall Friction	0.32
Particle Surface Adhesion	0
Number of Segments	8
Length per Segment (m)	1
Stress Precision Index	9

* Estimate only as initial simulation was run between site visit 2 and 3.

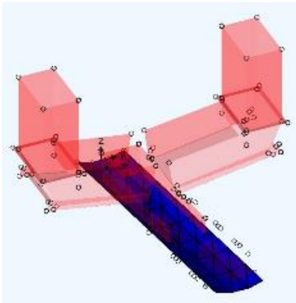

Figure 5-6 Belt

Chutes

Three chutes were created to allow for different simulation setups. All chutes were given the same initial parameters. The three chutes represent the skirts, feeder side plates and hopper discharge height and a labelled Chute_Skirts, Chute_Feeder and Chute_Hopper respectively. The initial coefficient of friction was set at 0.5 as per the discussion in section 2.3.4.

Table 5-4 Initial Chute parameters

Component Name	**Existing_Chute**
Time on (s)	-1
Time off (s)	5000
Wall Friction	0.5
Particle Surface Adhesion	0
Stress Precision Index	1
Tessellation Tolerance	3

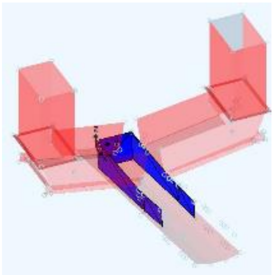

Figure 5-7 Skirts

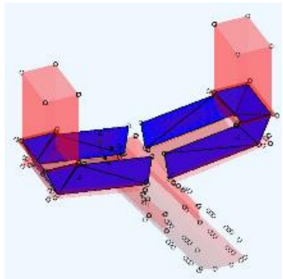

Figure 5-8 Feeder

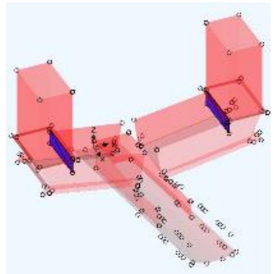

Figure 5-9 Hopper

The hopper height is the opening height of the hopper onto the feeder as seen in Figure 5-10.

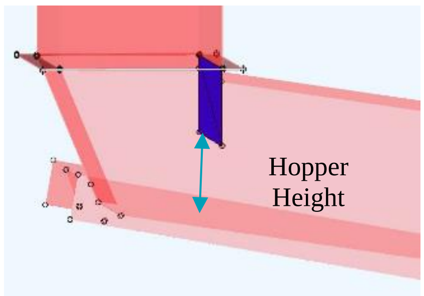

Figure 5-10 Hopper Height

Material properties

The initial material properties were identified as were as per the discussion in section 3.4.1.

Table 5-5 Initial material parameters

Material Name	**Ore_SS40_R**
Bulk Density (kg/m^3)	1900
Packing Ratio	1.5
Particle Density (kg/m^3)	2850
Conditions	Rough
Interparticle Friction	0.3
Particle Size Distribution	Random
Max Radius (mm)	40
Min Radius (mm)	40
Cohesive Condition	Slightly Sticky
Interparticle Cohesion	0.1596
Radius of Fines	0.9547

5.2.3 Determine Maximum Velocity

Effective model height was measured at approximately 3000 mm, giving a maximum possible velocity of due to gravity of 14.72 m/s. Therefore the Max Velocity for the simulation will be set at 15 m/s. The remaining simulation parameters were set as follows:

Table 5-6 Initial simulation parameters

Simulation Name	**FP_Original_1**
Simulation Time (s)	20
Max Speed (m/s)	15
Time Step Multiplier	1
Snapshot Frequency (frames /sec)	15
History & Force Output Frequency (frames/sec)	20

The resulting analysis run by BFA showed a maximum velocity of 29.81 m/s. An investigation into this result showed that the mass flow was not balanced causing particle build up in the injection box as shown in Figure 5-11. This build up caused particles to be created over existing particles resulting in particle explosions of high velocity.

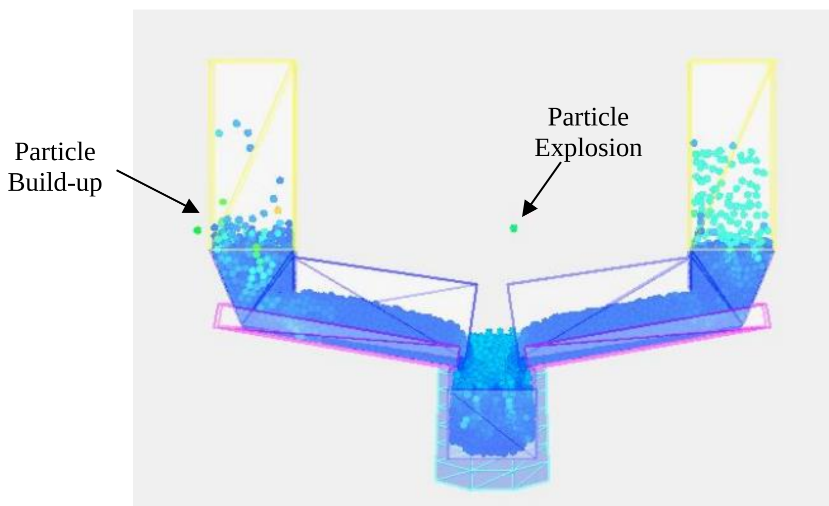

Figure 5-11 Material build up and particle explosion.

Review the simulation showed that particle build-up reached the base of the injection box at approximately 11 seconds into the simulation. Maximum velocity up to this time was 7.71 m/s.

For simulation FP_Original_2, the feeder speed was increased to 3.7 m/s and the max velocity for the simulation was reduced to 9.5 m/s as seen in Table E-8. Analysis of the simulation showed the maximum velocity was 8.24 m/s.

Maximum velocity for simulations will be set at 9.5 m/s.

5.2.4 Determine Minimum Particle Size

The Table 5-7 below summarizes the information in Table E-8 Appendix E against the predicted number of particles and time required determined by the equations described in section 2.3.2.

Table 5-7 Particle Size

Simulation	Particle Radius (mm)	Calculated Peak Particle Count	Actual Peak Particle Count	Calculated Simulation Time (minutes)	Actual Simulation Time (minutes)
FP_Original_2	40	-	9,102	-	34.38
FP_Original_3	15-12	172,600	< 250,000	1738	< 827.21
FP_Original_4	20-18	72,816	103,508	550	539.26
FP_Original_5	22-20	60,680	54,707	375	276.12

As can be seen an underestimation of the number of particles and an over estimation of the time to run was given by the prediction equations. The results however are skewed by the fact the radius range was used which would effectively increase the number of particles and time to run the simulation.

For future simulations a particle radius of 40 mm will be used to check simulation setups, with particle radius range of 20 mm to 22 mm used for comparative analysis.

5.2.5 Test Friction of Belt

The images below show the back flow at the impact zone for the belt coefficient of friction of 0.32 and 0.5 in comparison to a recorded image of the impact zone.

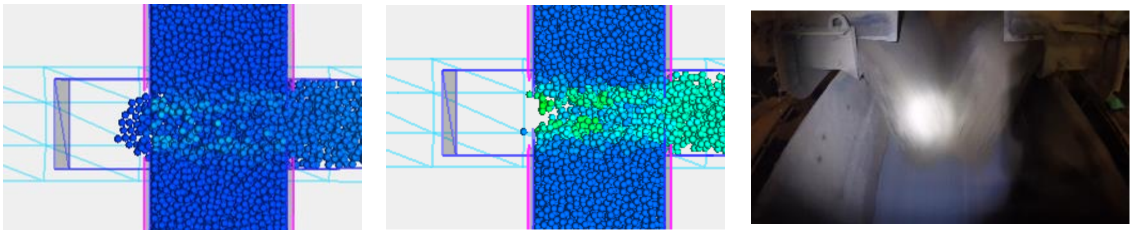

5-12(a) Belt Friction 0.32 *5-12(b) Belt Friction 0.5* *5-12(c) Record Transfer*

Figure 5-12 Belt Friction Analysis

As can be seen the 0.5 friction coefficient better represents the back flow of the material.

5.2.6 Mass Balancing

Due to uncontrolled circumstances the primary method for mass balancing the material flow is no longer available. As such mass balance was approximated by monitoring the hopper level at the feeder inlet. As seen in Figure 5-13, if the hopper level moved up into the injection box, then feeder speed was too slow and if the hopper level dropped below the hopper outlet height the feeder was too fast. Table E-9 and Table E-11 in Appendix E indicates which simulations were mass balanced, with a comment on the feeder speed if not mass balanced.

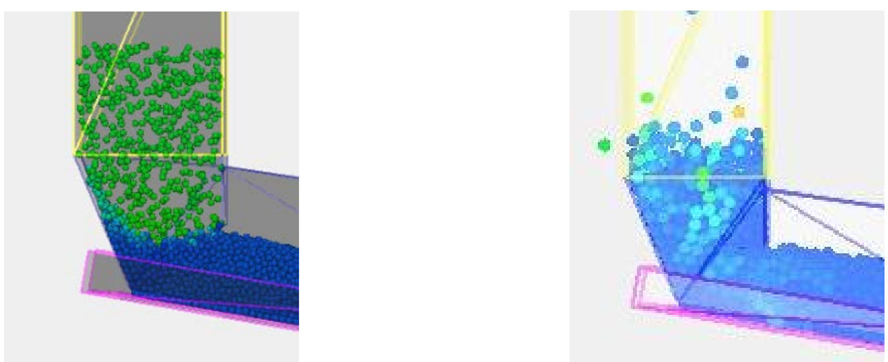

5-13(a) Feeder too fast *5-13(b) Feeder too slow*

Figure 5-13 Mass Balancing

5.2.7 Simulation Rating

To determine the accuracy of the simulation relative to the recorded transfer operation, each simulation was rated on how well the simulation replicated: 1) The final ore profile on the belt; and 2) How well it replicated the slumping action on the feeder. These two aspects of the simulation were chosen as they are key causes of the surging issues identified in section 5.2.1. A rating system of poor, marginal and good was used as seen in Figure 5-14 to Figure 5-16 show the differences between the materials spread ratings. Slumping action of the material was more subjective and required viewing of the simulation frame by frame to identify the generation of fracture lines.

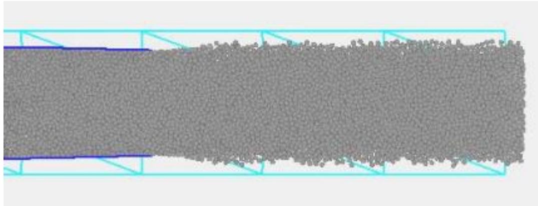

Figure 5-14 Good Material Spread

Material spreads out past the skirts and material profile on belt is flat.

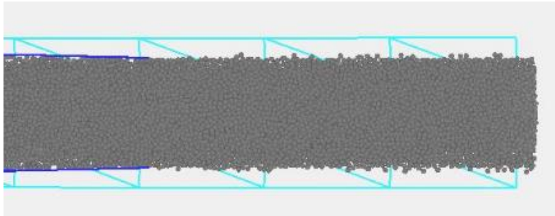

Figure 5-15 Marginal Material Spread

Material has some minor spreading past skirt with a good material profile on belt.

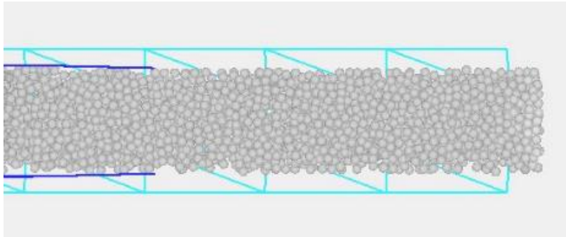

Figure 5-16 Poor Material Spread

Material does not spread past skirts and material profile on belt is lumpy without uniform shape.

Figure 5-17 Actual Material Spread

Still image of material spreading as it leaves the skirts.

5.2.1 Simulation Configuration

Two configurations of the simulation where run, the first shown in Table E-8 was a basic set up where the far side injection box starting at the beginning of the simulation followed with the near side injection box starting at 3 seconds after the start of the simulation. The second configuration shown in Table E-10 delayed the feeder start times as well by 3.9 and 13.9 seconds of simulation time respectively. This allowed a more instantaneous dumping of material onto RC01 rather than a ramping up effect seen with the basic configuration as seen in Figure 5-18, thus allowing a quicker development of steady state flow.

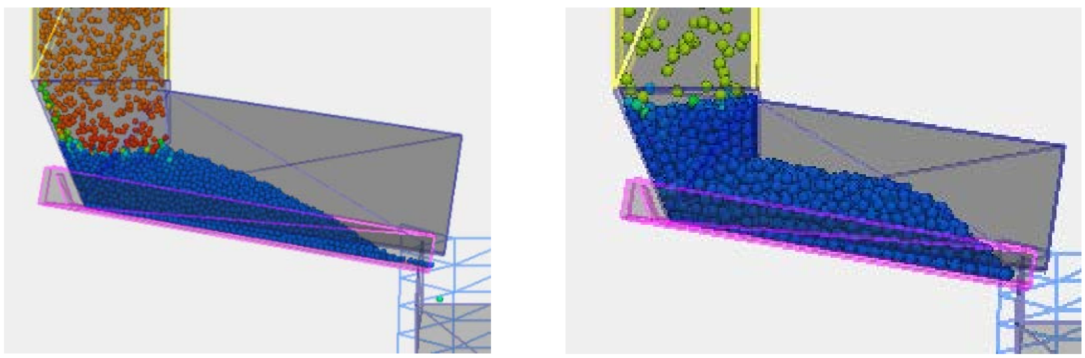

5-18(a) Basic Configuration *5-18(b) Delayed Configuration*

Figure 5-18 Basic and Delayed Configurations Bed Depth

5.3 Material Parameters

The material was recorded displaying some distinct behaviour in two locations during the site visits. Firstly the slumping action as it came off the end of the feeder, and then the spreading action as it exited the skirts. A series of simulations were run with varying material properties to attempt to replicate this behaviour. Using a rating system developed in section 5.2.7 each variation was compared to the actual material behaviour seen during the site visits. Two parameters were focused on, cohesion and inter-particle friction with the results were recorded in Table E-9.

5.4 Results

From Table E-9 and Table E-11 it can be seen that any form of cohesion added to the material caused good slumping action but poor spread of the material on the conveyor. The dry particles with a coefficient of cohesion of 0.00 typically showed good material spread but marginal to no slumping. In general it could said that increasing the cohesion coefficient increased the slumping action but decreased the materials ability to spread on the conveyor. Custom coefficients of friction were also trailed by including a radius of fines with little to know coefficient of cohesion as seen in simulations FP_Original_23/24/26. Comparison between FP_Original_20 and FP_Original_26 showed little to no difference in material spread and slumping action.

When adjustment of the inter-particle friction was conducted, Table E-9 and Table E-11 show that good slumping action was seen with high coefficient of friction values while good spreading action was seen with low coefficient of friction values.

The best parameters used to simulate the actual material flow where found by setting coefficient of cohesion to 0 and the inter-particle friction coefficient to 0.2 or 0.3. Therefore it is recommended that for each analysis two simulations be run, one at 0.2 inter-particle friction and one at 0.3 inter-particle friction. By using the two inter-particle friction coefficients, a more accurate picture of the inserts performance can be developed.

It was also discovered that when the material radius changed a recalibration of the mass balance was required. This was likely due to the better packing advantage smaller particles have over larger particles.

Investigation of the issues noted in section 5.2.1 had some success. When using a material with and inter-particle friction coefficient of 0.3 the simulation showed excellent non-central loading characteristics as seen in the comparison in Figure 5-19. Additionally back flow issue was suitably replicated section 5.2.5 by adjusting the belt friction. Further analysis will be conducted into this in Chapter 7.

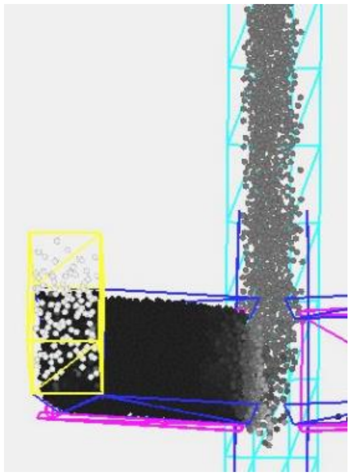

5-19(a) Simulation FP_Original_22

5-19(b) Recorded

Figure 5-19 Comparison of non-central loading

At the time of writing this report, the issue of surging was unfortunately not able to be sufficiently replicated using this simulation configurations identified in Appendix E. Several variations of the coefficients of inter-particle friction and cohesion were run and although slumping action of the material could be effectively replicated, it came at the expense of material spread when exiting the skirts.

5.5 Conclusion

A simulation was run based on the data provided collected from the site inspections as noted in section 3.6. Although at the initial running some data from the third site visit was not available, the simulation was used to determine some of basic parameters that will be used for all subsequent simulations. The following parameters set:

- Simulation maximum velocity of 9.5 m/s.
- Minimum particle radius size range of 20 mm - 22 mm.
- Testing simulations using a radius of 40 mm are to be used for quick analysis.
- Conveyor friction coefficient of 0.5.
- Method of mass balancing by adjustment of feeder speed.

Next a series of simulations where run to identify the best material parameters specifically focusing on the coefficients of cohesion and inter-particle friction. The results of these simulations highlighted two material configurations with coefficient of cohesion to 0 and the inter-particle friction coefficient to 0.2 or 0.3. Inter-particle friction coefficient to 0.2 provided good spreads of material while a coefficient to 0.3 provided good simulation of non-central loading of the material. At the time of writing this report, the issue of surging was unfortunately not able to be sufficiently replicated using this simulation configurations identified in Appendix E.

Finally it should be noted that a modelling error was discovered that set the height of the hopper at 700 mm instead of the required 600 mm. Simulations were re-run with the preferred material properties at 600 mm hopper height and all data is recorded in Appendix E.

Chapter 6 Improved Transfer Chute Design

This chapter will review the results of the existing and improved chute simulations and report on the comparative differences between the two designs.

6.1 Introduction

Three designs options were trialled to resolve the noted issues of material flow. The first was a traditional styled insert where the angle sides direct the material towards the centre of the belt, the second was an angled extension of the feeder beds and the third was a combination of both the traditional style and feeder extension. Each design was modelled and a simulations where run to determine its viability as a solution for the identified issues in section 5.2.1.

All designs are significantly restricted by the height between the feeders and the belt. Additionally a variety of material types are handled by this transfer station. For this reason rock boxes where not considered and the design will be based around side wall angles of 70° minimum from horizontal.

6.2 Chute Modification Option 1

The first design option was developed to address both the non-central loading and poor material profile development while having minimal impact on the existing skirting system. In addition to these design requirements, there were additional limiting factors that restricted the design options. These factors include the long discharge face of the feeders and low material velocity which negated the viability of a hood and spoon type chute. Another issue is the low height of 600-800 mm between the feeder outlets and the sloping conveyor belt which gave limited options for conventional material flow control methods through chute geometry. Additionally the low discharge height and low material discharge velocity results in an overall low material velocity through the chute, negating the requirement of any design measures associated with this and increasing the chance of material blockages through flow restrictions.

The resulting design was developed based on a load-out chute design as seen in Figure 2-5 that can be inserted within the existing skirting arrangement. The two requirements for this type of design include an angled side wall to centralise the material onto the belt and a diverging opening to allow the development of a good material profile. The load-chute divergence will be set at 300 mm at the back of the insert to a 560 mm opening at the outlet over a length of 2000 mm. This design coupled with the arrangement restrictions dictated the a side wall slope of 70° from horizontal and the back wall set at 80° from horizontal to maintain a valley angle of greater than 70°. The final design is shown in Figure 6-1.

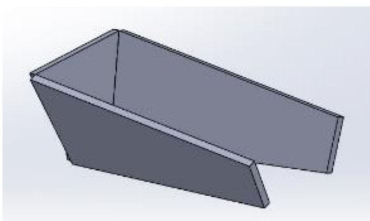

6-1(a) 3D Model

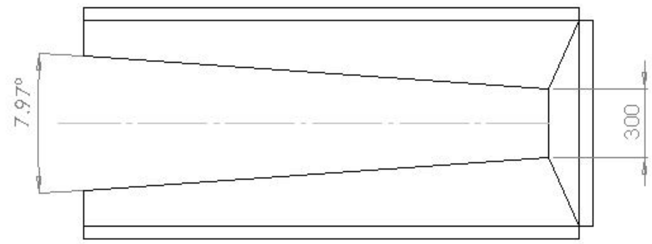

6-1(a) Dimensions

Figure 6-1 Insert Created in SolidWorks

A thickness of 60 mm was added to represent the expected thickness of the liners plates, insert wall plates and any stiffeners required for support. Figure 6-2 shows how the insert sits inside the BFA simulation model.

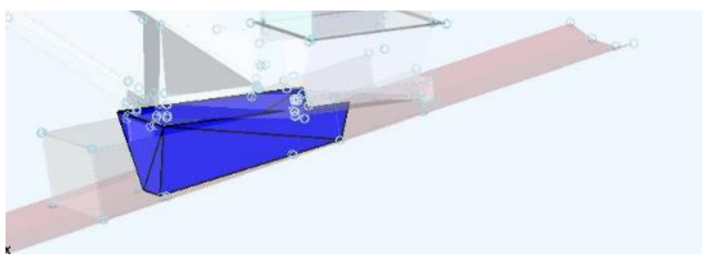

Figure 6-2 Insert Positioned in BFA Model

6.2.1 Simulation Configuration of Option 1

Table E-14 shows the configurations for the three simulations run. The first two simulations, FP_ Insert_1 and FP_ Insert_2, trialled material Ore_D40_S and Ore_D40_R respectively. For simulation FP_ Insert_3 the insert divergence was increased from 300 mm and 560 mm to 350 and 610 mm.

6.2.1 Simulation Results of Option 1

As can be seen by Figure 6-3, the insert caused a blockage in the impact zone. This was typical for all three simulations run.

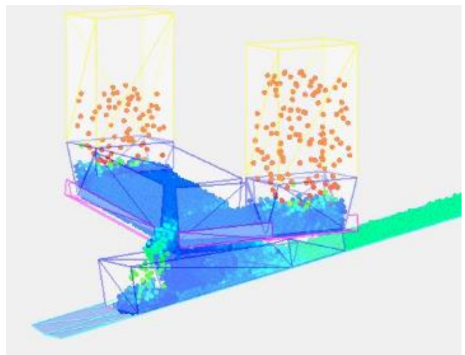

Figure 6-3 Simulation of Option 1

6.3 Chute Modification Option 2

Due to the failure of option one in attempting to rectify both non-central loading and material profile simultaneously, option two would be simplified by only focussing on the non-central loading. For this option a simple tapered extension to the feeder was modelled as seen in Figure 6-4. The taper is set so that there was a minimum 350 mm gap between the two feeders to allow material to be discharged onto the belt centre. The rationale behind the extension was to discharge the material from the feeder onto the centre of the conveyer rather than directing the flow post discharge from feeder. The tapering of the extensions was to provide some material profile development in a similar manner to the divergence in a traditional load-out chute.

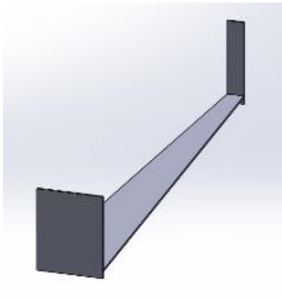

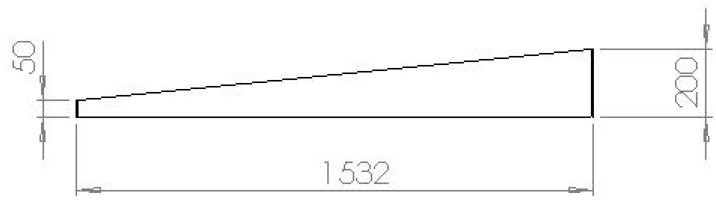

6-4(a) 3D Model *6-4(b) Dimensions of Taper*

Figure 6-4 Tapered Extension

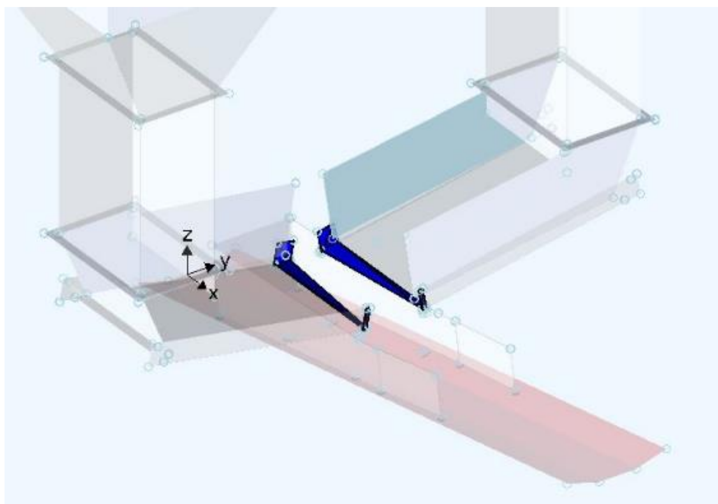

Figure 6-5 Extension Positioned in BFA Model

6.3.1 Simulation Configuration of Option 2

Table E-15 shows the configurations for the three simulations run. The first simulations, FP_Orig_Ext_1 trialled material Ore_D40_S and was successful. Simulation FP_Orig_Insert_2 and FP_Orig_Insert_3 was then run with material Ore_D22_S and Ore_D22_R respectively.

6.3.1 Simulation Results of Option 2

The simulation FP_Orig_Ext_1 was successful and did not cause any blocking. Initial findings showed that improved the centralisation of the load on the conveyor as seen in Figure 6-6.

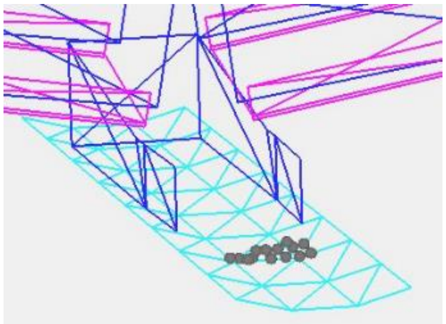

6-6(a) FP_Original_21

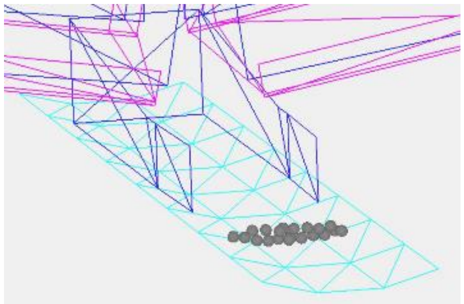

6-6(b) FP_Orig_Ext_1

Figure 6-6 Material Profile Comparison Showing Improved Load Centralization Profile View

Figure 6-6(a) shows the base line simulation, with material build up to one side of the belt. In Figure 6-6(b) the material is loaded centrally with a more uniform profile. The material used in this comparison had a low inter-particle friction coefficient causing it to spread across the belt easily. The effect of this spread would potentially hide the improved load centralisation.

Figure 6-7 shows a similar comparison with smaller radius particles and high inter-particle friction coefficient. Here the improvement can be seen with a greater gap present between Figure 6-7(b) compaered to Figure 6-7(a).

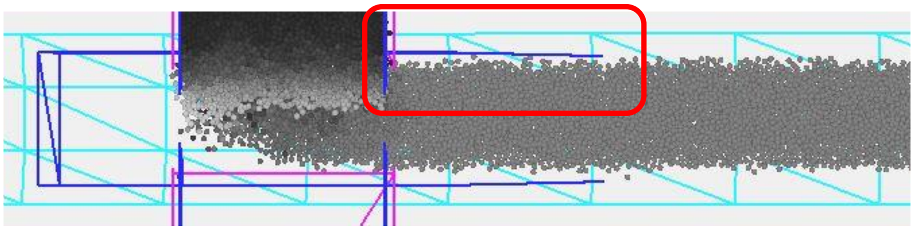

6-7(a) FP_Original_20

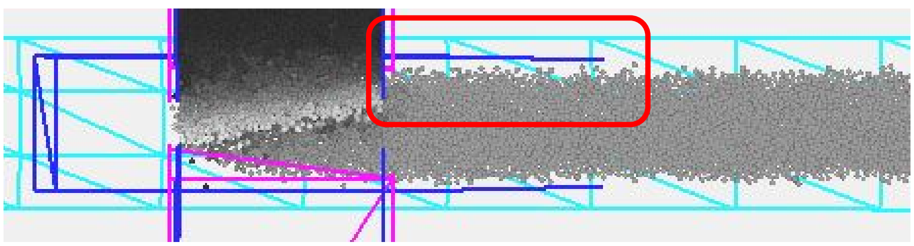

6-7(b) FP_Orig_Ext_3

Figure 6-7 Material Profile Comparison Showing Improved Load Centralization Top View

When both feeders were operating there appeared to be no restriction in the flow through the transfer.

6.4 Chute Modification Option 3

Due to the success in centralising the material onto the receiving conveyor, option three was created to improve the material profile development. Option three combined the tapered extensions modelled as seen in Figure 6-4, with a vertical walled insert shown in Figure 6-8. The benefit of this combination of tapered extension and insert is that it allows the insert to have vertical side plates, thus removing the potential of material building up the sides of the insert. An angled back plate of 80° to horizontal was kept and the divergence was modified from 440 mm at the back to a 750 mm opening at the outlet end.

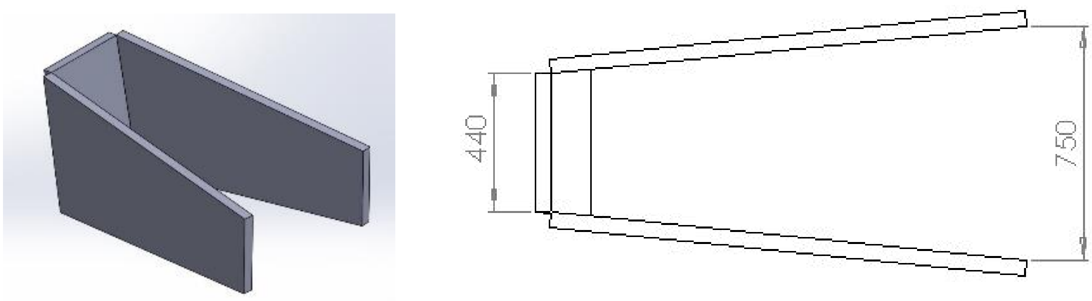

6-8(a) 3D Model *7-8(b) Dimensions*

Figure 6-8 Insert Option 3, Vertical Sides with 80° Angled Back

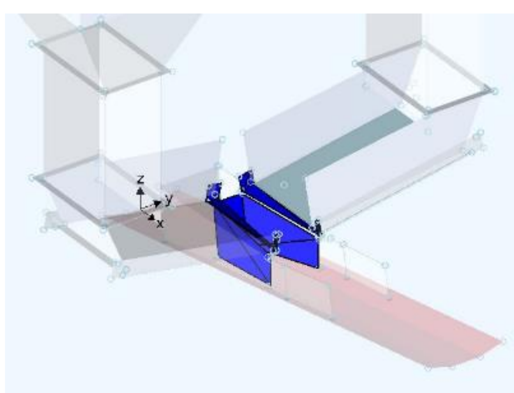

Figure 6-9 Extension and Insert Positioned in BFA Model

6.4.1 Simulation Configuration of Option 2

Table E-16 shows the configurations for the four simulations run. The first two simulations, FP_Orig_Ext_4 and FP_Orig_Insert_5 trialled material Ore_D40_R and Ore_D40_S respectively and was successful. Simulation FP_Orig_Insert_6 and FP_Orig_Insert_7 was then run with material Ore_D22_R and Ore_D22_S respectively.

6.4.2 Simulation Results

The most significant result from this simulation was that the chute insert did not cause a blockage as in section 6.2. Overall the simulations were a success and the results of the simulations are shown in Table E-16 with clear improvements in the material profile.

Figure 6-10 shows four images of the material profile after the material has left the skirts. Figure 6-10(a) shows the base line simulation, Figure 6-10(b) is the with the feeder extensions only while Figure 6-10(c) and Figure 6-10(d) include the insert and feeder extensions. Figure 6-10(a), Figure 6-10(b) and Figure 6-10(c) used Ore_D22_R material while Figure 6-10(d) used Ore_D22_S material.

There was an improvement in the material profile using the insert as seen in Figure 6-10(c) and Figure 6-10(d) when compared to Figure 6-10(a) and Figure 6-10(b) which had a flatter less rounded upper section of the profile. Additionally Figure 6-10(d) shows a greater spread across the conveyor belt compared to Figure 6-10(c).

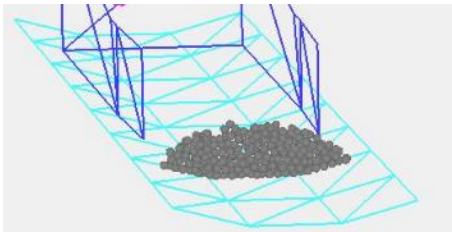

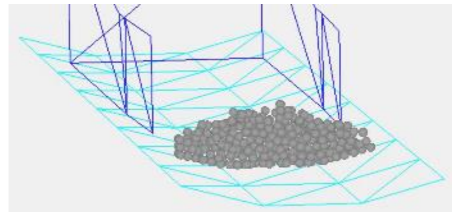

6-10(a) FP_Original_20 *6-10(b) FP_Orig_Ext_3*

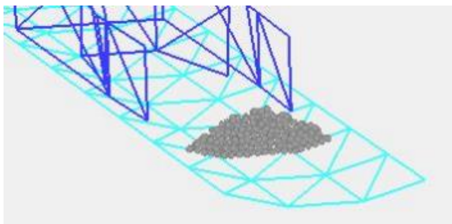

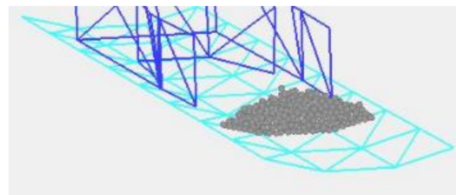

6-10(c) FP_Orig_Ext_6 *6-10(d) FP_Orig_Ext_7*

Figure 6-10 Material Profile Comparison Showing Improved Material Profile

6.5 Conclusion

Of the three options, option three showed the best improvement in centralising the material load and formation of the material profile on the belt. Option one suffered a severe blockages and an additional modification chute size had no impact on the result. Option two showed an improved load centralisation compared to base line simulation with little to no improvement in the material profile.

The angled side plates used in inserts for option one slowed the material velocity and allowed material build-up on the side plates, increased belt speed may help remove material faster out of the insert reducing the build-up on the side plates, however this modification defeats the purpose of adding the insert as it removes the possibility of increasing the flow rate. The real benefit from the blocked chute outcome is that it shows that angle side plates pose a risk for chute blockages.

Option two showed success in improving the load centralisation, however there was marginal control provided for the formation of the material profile. The simulation was successful in showing this effect with the profile exiting the skirts having a flat top section as opposed to the desired rounded profile. It should also be noted here that no calculations have been undertaken to prove the feasibility of extending the feeders in this manner. It is likely that this modification will place significant additional loads on the support structure and may affect its balance during operation. It does however highlight that it is worth investigating as a possible modification.

Option three combined the benefit of centralising the loading with control of material profile development. The feeder extensions allowed the insert to have vertical side plates instead of the angle as in option one preventing the material build up on the plates and could be easily removed by the conveyor.

Chapter 7 Conclusion and Further Work

This final chapter deals with the achievements, conclusions, recommendations and further work required to improve the transfer chute at Kwinana Bulk Terminal. It will also conclude this project.

7.1 Achievement of Project Objectives

From the original specification as provided in Appendix A, the majority of objectives were met except for:

- Development of suitable testing equipment for determining sample properties.
- Analysis of DEM model for areas of wear.
- Checking the improved chute design with a more cohesive material.

The project was successful in:

- Identifying a suitable Chute for analysis.
- Modelling existing chute.
- Confirming the DEM simulation matches real life material behaviour.
- Development of new chute design to resolve simulated issues.
- Confirmation of success of the new design in resolving simulated issues using DEM design.

7.2 Conclusion

A background investigation was conducted into some of the common issues and current transfer chute design methods that resolve those issues. This also covered a detailed description of the port facility at Kwinana Bulk Terminal run by Fremantle Port Authority and the specific transfer chute this project was based upon.

Three site trips where conducted to identify issues of poor design in the existing chute and to collect data for creation of the 3D model and initial parameter settings for DEM configuration. The first visit identified a number of issues, many of which are interrelated. Some issues were not able to be simulated by the DEM software supplied. As such, three issues were identified as being resolvable by the DEM software:

- Non-central loading
- Back flow
- Surging

The second and third site visit were primarily focused on recording data for building the models for simulation. Although this was an overall success, there were some issues with quality of the data that were noted such as exact details of vibratory feeder and poor recording setup. Additionally conveyor concavity, hopper opening size and belt transition were not accurately determined and therefore not included in the model for the DEM simulation.

Solidworks was chosen as the preferred software due to its parametric modelling capability, and availability of software integration support through Overland Conveyor Inc. Rationalisation of the recorded data meant that the belt transition, belt concave curvature where feeder length where not exactly replicated in the 3D model. This was not expected to significantly impact the results as this is a comparative analysis of transfer chute performance.

A simulation was run based on the data collected from the site inspections was run and the following a set of basic parameters identified for all future simulations such as iteration step size, minimum particle size and a method of mass balancing the simulation. This was then followed by a number of simulations to determine the best material parameters with the result highlighting two material configurations. These two materials provided good simulation of non-central loading and material spread when exiting the conveyor skirting. At the time of writing this report, the issue of surging was unfortunately not able to be sufficiently replicated using this simulation configurations identified.

Limiting factors that restricted the design options associated the equipment arrangement were identified. These factors include the long discharge face of the feeders, low height between the feeder outlets, the sloping conveyor belt and low material velocity through the chute. This removed many potential solutions for controlling the material flow and added complexity to the resulting designs.

Three chute design options where developed to resolve the identified issues of non-central loading and poor material profile development that fit within the existing equipment arrangement restrictions. Of the three options, option three showed the best improvement in centralising the material load and formation of the material profile on the belt. Option one suffered a severe blockages as material appeared to slow and build-up on the insert side walls resulting in the chute blocking. Option two showed an improved load centralisation compared to base line simulation with little to no improvement in the material profile.

Option three combined the benefit of centralising the material loading with control of material profile development. This option included feeder extensions to centralise the loading of the material and then used an insert with vertical side plates to control the material flow such that it formed the desired material profile on the conveyor belt.

The real benefit from the blocked chute outcome in option one and the poor profile development in option two was that it showed that the simulation is capable of predicting potential issues with transfer chute design. However due to the significant variation between the DEM model and the actual transfer station as well as the inability to replicate the slumping effect that caused the material surging, DEM should not be the only tool used to verify designs. Scale modelling and conventional chute design still play an important role in good design.

7.3 Further Work

There still remains further investigations to be carried out to improve the confidence of the chosen chute design. The following additional work is recommended to resolve some of the issues not yet addressed by this project:

- Further investigation of the surging issue. As material properties could not be set such that they replicated the surging effect recorded during the site visits, it cannot be conclusively proved that the new chute design will function without blocking. However by manipulating the material flow through the model a simulation of the surging effect can be achieved. This ca be done by using additional material injection boxes that add material onto the feeder bed at regular intervals.
- Other variations of chute inserts can be trialled to attempt to remove the feeder extension component of the chosen chute design. Extending the feeder beds in this manner is likely to substantially change the dynamics of the feeder operation and require further engineering investigation into its feasibility. Alternate methods of centralising the material that do not require such significant modification to the feeders may be available.

- Investigation into the effect the new chute designs has on belt wear. The BFA software provides a method for investigating belt wear caused by particle impact and friction. Although the software does not give a specific numeric value to depth and rate of belt wear, it does provide a numeric value to the intensity of the impact of the particles onto the belt. The software also provides an estimation of the gouging caused as a function of pressure and the relative motion between the particle and belt. These numbers can be used comparatively to provide an indication on whether one chute design protects the receiving belt form wear more effectively then another.
- Running the DEM model with a variation of material properties. The BFA software has a large number of material property variations that can be set including particle clusters. There is merit in testing the chosen chute design with a variety of different materials, such as cohesiveness and particle shape, to ascertain the limits of the chutes capacity to handle a variety of products.
- Simulating the vibrational action of the feeder to ascertain if this has any impact in the flow behaviour of the material. The simulations run for this project only gave a surface velocity to the feeder beds, parallel to the material flow direction. The BFA software does provide a method of creating a vibrating surface for the purpose of simulating the action of vibratory feeders.

References

Andrew L. Mular, Doug N. Halbe & Barratt, DJ 2002, *Mineral Processing Plant Design, Practice and Control*, vol. 2, Society for Mining, Metallurgy, and Exploration, Inc., Littleton, Colorado USA.

Arnold, PC 1980, *Bulk solids : storage, flow and handling*, 2nd ed. edn, TUNRA Bulk Solids Handling Research Associates, Newcastle NSW.

Beckley, D 2011, Belt Conveyor Transfer Chutes - Tips for Designers, Australian Society for Bulk Solids Handling, 17 October 2011.

Benjamin, C, Donecker, P, Huque, S & Rozentals, J 2015, *The Transfer Chute Design Manual for Conveyor Belt Systems*, Conveyor Transfer Design Pty Ltd.

Bharadwaj, R 2012, 'Using DEM to solve bulk material handling problems', *Chemical Engineering Progress*, vol. 108, no. 9, pp. 54-8.

Bulk Flow Analyst, 2016, Overland Conveyor Company INC, Lakewood.

CEMA 1997, *Belt Conveyors for Bulk Materials*, Conveyor Equipment Manufacturers Association, United States of America.

Cundall, PA & Strack, OD 1979, 'A discrete numerical model for granular assemblies', *Geotechnique*, vol. 29, no. 1, pp. 47-65.

Davis, S n.d., *Transfer Chute Design Fundamentals*, IIR Executive Development, Course Notes, <http://www.informa.com.au/training/instructor-profile/steve-davis>.

DEM Solutions Limited 2016, *EDEM Software*, DEM Solutions Limited, viewed 11 May 2016, <http://www.edemsimulation.com/software/>.

Derakhshani, SM, Schott, DL & Lodewijks, G 2013, 'Modeling dust liberation at the belt conveyor transfer point with CFD and DEM', in *11th International Congress on Bulk Materials Storage, Handling and Transportation, Newcastle*.

Favier, L, Daudon, D, Donzé, F-V & Mazars, J 2009, 'Predicting the drag coefficient of a granular flow using the discrete element method', *Journal of Statistical Mechanics: Theory and Experiment*, vol. 2009, no. 06, p. P06012.

Fremantle Ports Annual Report, 2015, Fremantle.
http://www.fremantleports.com.au/News/Publications/AnnualReport/Documents/2015%20Annual%20Report%20-%20Full%20Report.pdf>.

Grima, A, Hastie, D, Curry, D, Wypych, P & LaRoche, R 2011, 'The beginning of a new era in design: calibrated discrete element modelling', *Australian Bulk Handling Review*, vol. 16, no. 6, pp. 14-21.

Hastie, DB & Wypych, PW 2010, 'Experimental validation of particle flow through conveyor transfer hoods via continuum and discrete element methods', *Mechanics of Materials*, vol. 42, no. 4, pp. 383-94.

Hudson, C 2016, *Bulk Flow Analyst Workshop*, Applied DEM, Colorado.

Khambekar, J, Pittnger, B, Jenike & Johanson, Dandan, R & Dominion Resource Services 2015, 'Chutes and Suitability', *World Coal*, vol. 24, no. Issue, http://www.worldcoal.com/magazines/issue.aspx?seo=world-coal&month=8&year=2015>.

Langston, PA, Al-Awamleh, MA, Fraige, FY & Asmar, BN 2004, 'Distinct element modelling of non-spherical frictionless particle flow', *Chemical Engineering Science*, vol. 59, no. 2, pp. 425-35.

Nordell, LK 1997, 'Particle flow modeling: transfer chutes & other applications', in *Beltcon conference*.

Schwedes, J & Schulze, D 1990, 'Measurement of flow properties of bulk solids', *Powder Technology*, vol. 61, no. 1, pp. 59-68.

Swinderman, T, Marti, AD, Goldbeck, LJ, Marshall, D & Strebel, Mg 2009, *Foundations - The Practical Resource for Cleaner, Safer, More Productice Dust and Material Control*, Fourth edn, Martin Engineering Company, Neponset Illinois USA.

The Transfer Chute Design Manual, 2010, Forum, created by Wöhlbier, RH, Bulk-Online, viewed 11.5.2016, <http://forum.bulk-online.com/showthread.php?21113>.

Appendix A.

ENG4111/4112 Research Project

Project Specification

For: Alex Mason

Title: Improved Transfer Chute Design Using DEM Software to Predict Material Flow Behaviour

Major: Mechanical Engineering

Supervisor: Canh-Dung Tran

Enrolment: ENG4111-EXT S1, 2016
ENG4112-EXT S2, 2016

Project Aim: To develop a system for identifying chute performance issues and evaluating the proposed solutions using DEM software.

Programme: Issue A 14th March 2016

1. Identify suitable chute for analysis and video record existing chute operation. Obtain sample of the material that was transferred during recording.

2. Obtain/manufacture suitable testing equipment for determining sample properties.
    a. Sieving equipment.
    b. Rolling/Sliding friction tester.
    c. Dynamic angle of repose tester.

3. Set DEM material properties to match tested properties.

4. Model existing Chute.

5. Run DEM model and visually confirm model reflects real life operation.

6. Analyse data developed from DEM model to identify areas of wear, blockage, spillage and belt tracking.

7. Model AECOM chute design.

8. Run DEM model, and analyse data from DEM model to identify areas of wear, blockage, spillage and belt tracking.

9. Develop new chute design based on current best practice, focussing on issues noted in existing chute design.

10. Run DEM model, and analyse data from DEM model to identify areas of wear, blockage, spillage and belt tracking.

    If time and resources permit

11. Modify material properties to represent more cohesive material and re-run DEM model of new chute design. Analyse data from DEM model to identify areas of wear, blockage, spillage and belt tracking.

Appendix B.

Excessive Spillage

Figure B-1 Spillage adjacent to chute outlet.

The spillage shown here is directly adjacent to the chute outlet.

This indicates that either is an issue in the control of the transfer chutes loading pattern or an indication of belt tracking issues.

Additionally there have been reports of material surges that cause spillage related to overflow.

<table>
<tr><th colspan="2">Belt wear</th></tr>
<tr><td>
Figure B-2 Longitudinal wear lines.</td><td>The longitudinal lines seen running length wise on the conveyor belt indicate that some wear is occurring on the belt surface during operation.

Some operational wear of the belt surface is always to be expected however this issue will still be investigated.</td></tr>
</table>

<table>
<tr><th colspan="2">Belt Lift</th></tr>
<tr>
<td>


Figure B-3 Belt lift

Figure B-4 Flattening of belt at chute outlet.
</td>
<td>
The belt is lifting off the surface of the centre idler due to a combination of concave curvature the conveyor and high belt tension.

The resulting flattening of the belt will add to the inability of the transfer chute to develop a stable loading pattern, hence adding to spillage issues.
</td>
</tr>
</table>

<table>
<tr><td colspan="3">Belt Alignment</td></tr>
<tr><td>
Figure B-5 Tail pulley, left side.</td><td>
Figure B-6 Tail pulley, right side</td><td>The belt is tracking significantly to the right side on the tail pulley.

This can have multiple simultaneous causes; however a specific relationship between this issue and the material loading pattern will be investigated.</td></tr>
<tr><td colspan="3">Non-Central Loading</td></tr>
<tr><td colspan="2">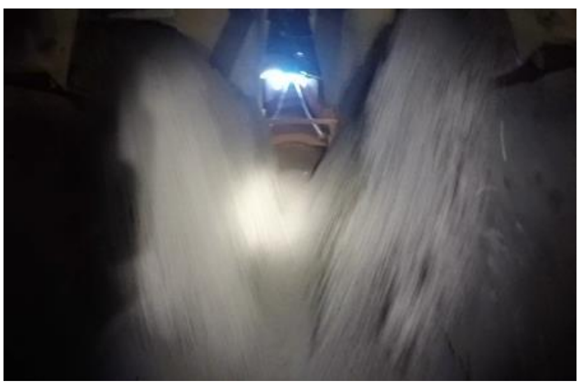
Figure B-7 View from tail end showing non- central loading on belt.</td><td>Non-central loading causes belt tracking issues. Depending on which feeder is loading the belt will track in to the opposite side as the loaded material centralizes on belt.</td></tr>
</table>

<table>
<tr><td colspan="2">
Figure B-8 One feeder in operation.</td><td>Again non-centralised loading of the conveyor belt, belt slip is evident by exposure of idlers on left hand side.</td></tr>
<tr><td colspan="3">**Lack of load profile on outgoing belt**</td></tr>
<tr><td colspan="2">
Figure B-9 Lack of load profile</td><td>Lack of load profile increases chance of spillage as the material is conveyed and reduces maximum capacity of belt.

Lack of profile is noticeable from horizontal shadow cast on material.</td></tr>
<tr><td colspan="3">**Back Flow**</td></tr>
<tr><td>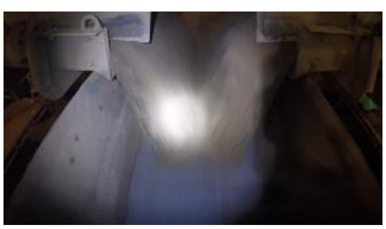
Figure B-10 No back flow</td><td>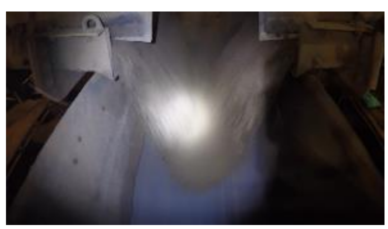
Figure B-11 Backflow</td><td>Material that flows or boils backwards causes increased wear on the belt.</td></tr>
<tr><td colspan="3">**Surging**</td></tr>
</table>

 *Figure B-12 Surging*	The waviness of the material seen along the edge of the conveyor belt is a result of the material slumping as it comes off the end of the feeder.

Slumping		
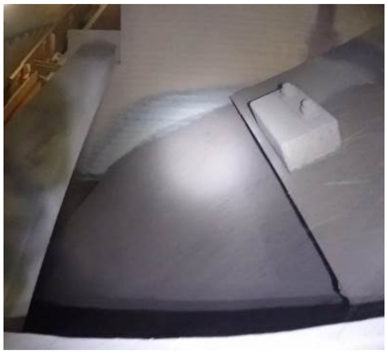 (a i) *Time 0.00*	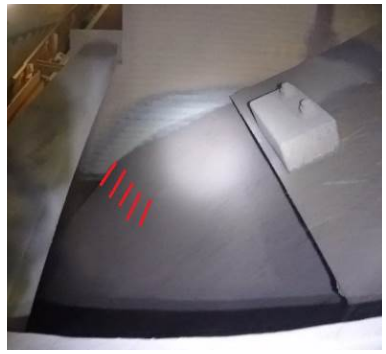 *(a ii) Discharge face.*	Slumping effect was noticed during feeder operation. Figure B-13(a ii) shows the discharge face.
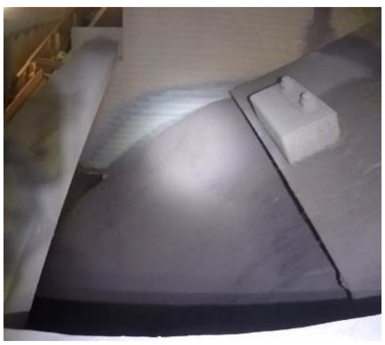 *(b i) Time 0.50*	 *(b ii) Fracture line*	Figure B-13(b ii) shows a new fracture line has developed behind the discharge face. The initial discharge face has fallen off the end of the feeder.
 *(c i) Time 1.00*	 *(c ii) New Discharge Face*	Figure B-13(c ii) shows a new discharge face developing as the material slumps down the fracture line.

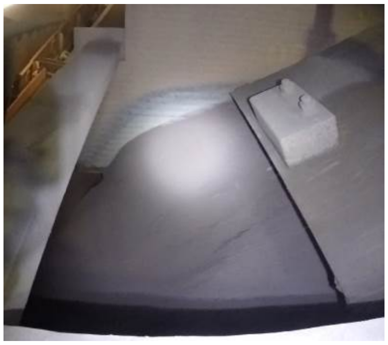 *(d i) Time 1.50*	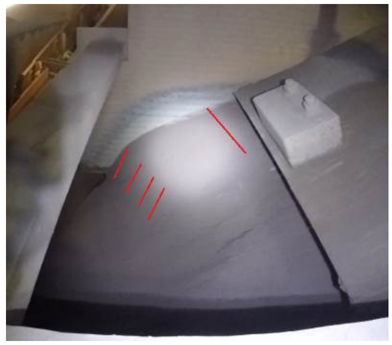 *(d ii) New Fracture Line*	Figure B-13(d ii) shows a new fracture line developing the behind the preciously created fracture face.
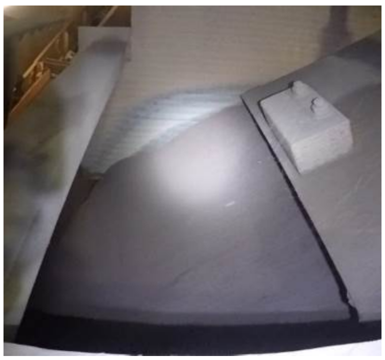 *(e i) Time 1.75*	 *(e ii) Slumping of Material*	Figure B-13(d ii) shows the material sliding or slumping down the fracture face in a large clump. As can be seen by Figure B-13 (d i) & (f i) that this slumping occurred within half a second.
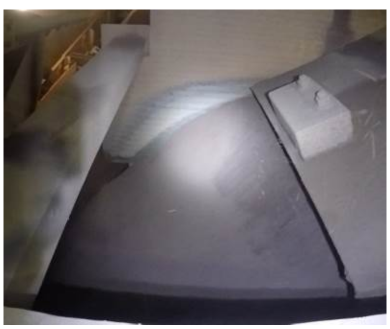 *(e i) Time 2.00*	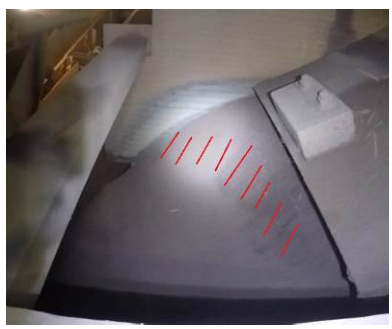 *(e i) New Discharge Face*	Figure B-13(e ii) shows a new discharge face developing as the material slumps down the fracture line.

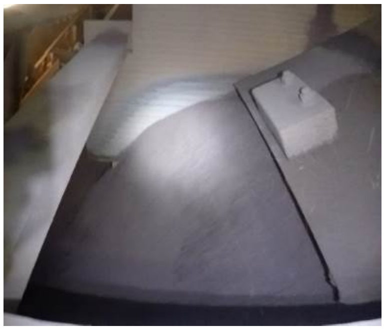 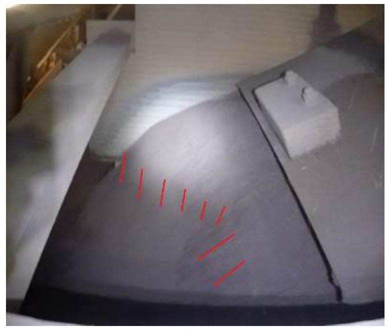 *(f i) Time 2.50* *(f ii) Cycle repeating* *Figure B-13 Material slumping action*	Figure B-13(f ii) shows the discharge face moving closer to end of feeder. This movement is facilitating the creation of the next fracture line, allow the cycle to repeat.

Appendix C.

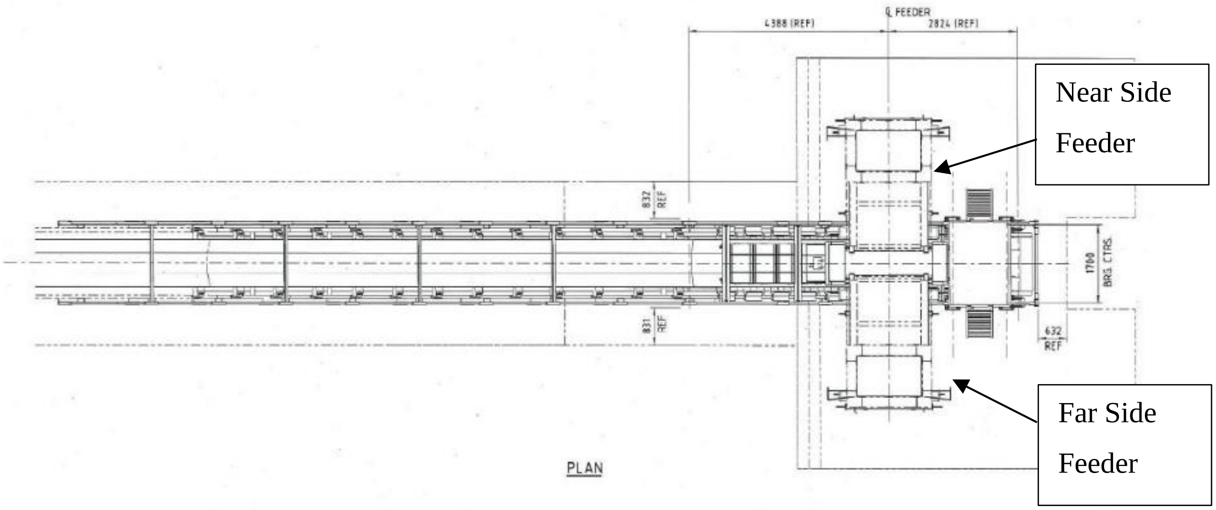

Figure C-1 Taken from Drawing 600196043-0100-ME-DRG-0001

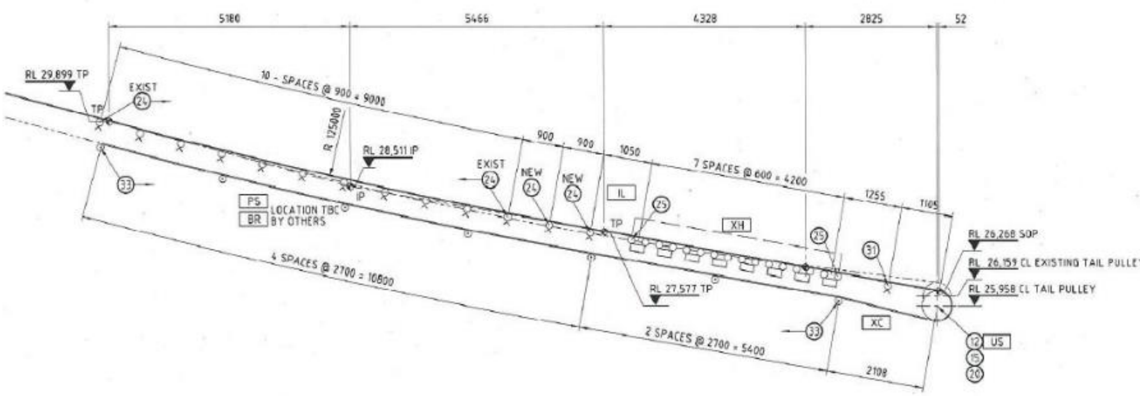

Figure C-2 Taken from Drawing 600196043-0100-ME-DRG-0002

Figure C-1 and Figure C-2 show drawings taken from a report produced by AECOM for a solution the belt lift issues and incorporates the new feeders recently purchased by FPA. The drawings show a complete rebuild for the tail end of RC01, however the general layout positions still remain relative to existing layout at KBT. Any specific chute improvement developed will need to still work with the new tail arrangement.

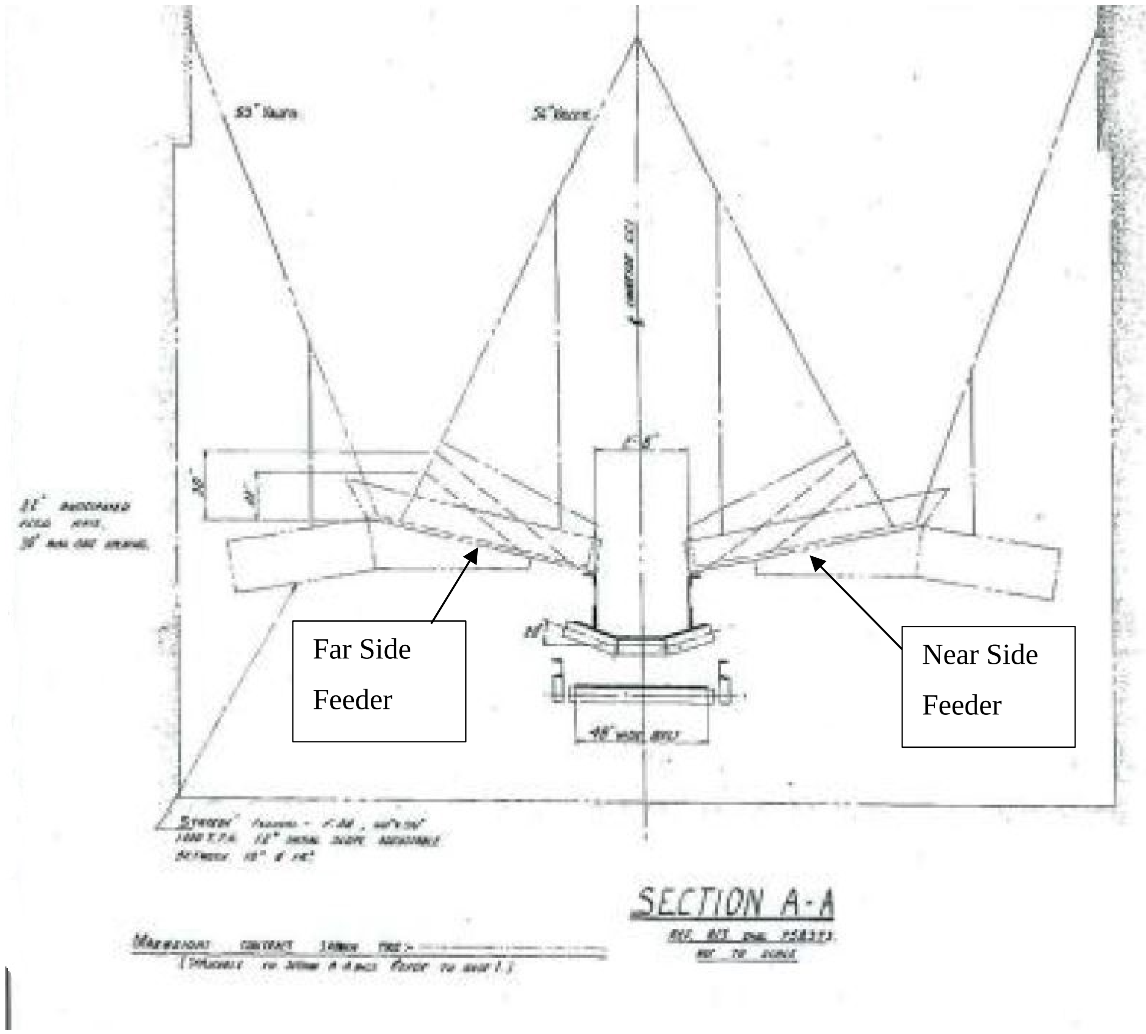

Figure C-3 Taken from Drawing K16350

Figure C-3 is taken from the original tail end arrangement drawing for RC01 and shows the cross section of bin, feeder and conveyor arrangement.

Appendix D.

Elevation of Feeder and Conveyor

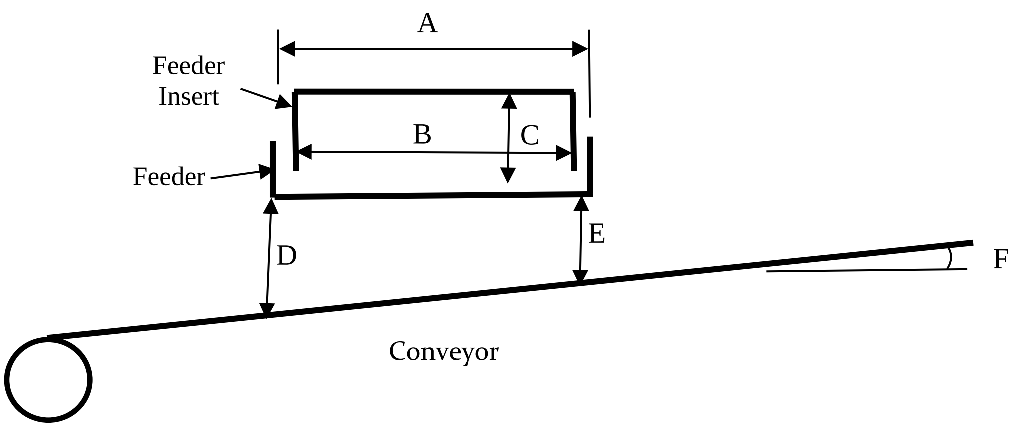

A	B	C	D	E	F
1520 mm	1398	-	800 mm	600 mm	10°

Plan of Feeder and Conveyor Skirt

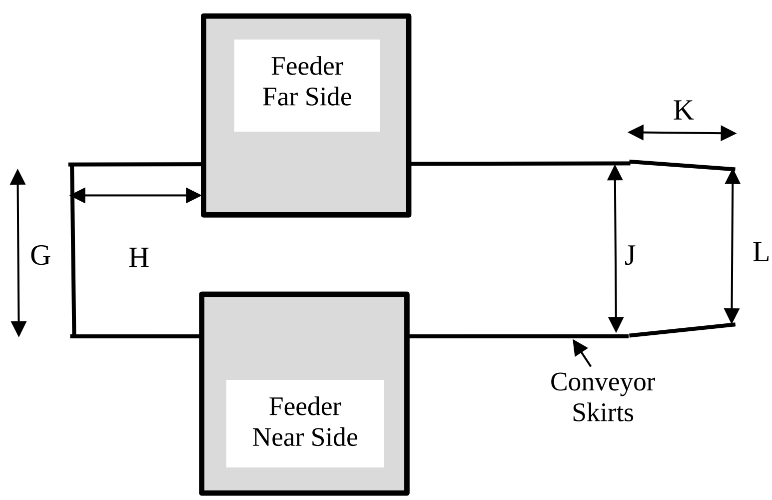

G	H	J	K	L
917 mm	660 mm	912 mm	1000 mm	864

Section of Feeder, Conveyor and Skirts

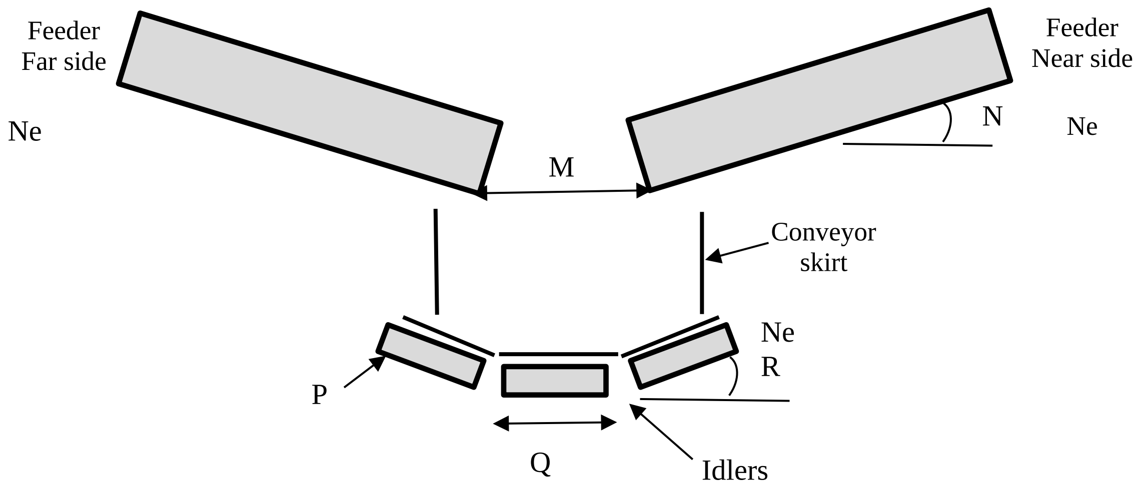

M	N	P	Q	R
755 mm	10°	Ø 152 mm	440 mm	15°

Side Elevation of Skirts

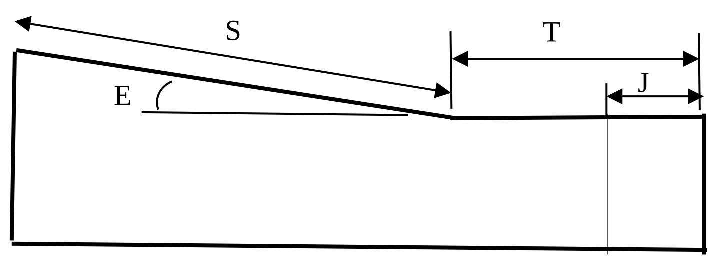

S	T
2540 mm	1300 mm

Appendix E.

Table E-1 Injection Boxes

Component Name	Inj_FS/NS_1300	Inj_FS/NS_1150	Inj_FS/NS_1150_Del
Time on (s)	-1	-1	-1
Time off (s)	5000	5000	5000
Inj Start (s)	0/3	0/3	0/10
Inj Stop (s)	20	20	50/50
Flow Rate (t/hr)	1300	1150	1150
Tessellation Tolerance	3	3	3

Table E-2 Conveyor Belts

Component Name	RC01_Fr0-32_S3-0	RC01_Fr0-5_S3-0	RC01_Fr0-5_S2-16
Time on (s)	-1	-1	-1
Time off (s)	5000	5000	5000
Velocity (m/s)	3	3	2.16
Wall Friction	0.32	0.5	0.5
Particle Surface Adhesion	0	0	0
Number of Segments	8	8	8
Length per Segment (m)	1	1	1
Stress Precision Index	9	9	9

Table E-3 Feeders for Basic Configeration

Component Name	Feeder_FS/NS_S27	Feeder_FS/NS_S28	Feeder_FS/NS_S30	Feeder_FS/NS_S36
Time on (s)	-1	-1	-1	-1
Time off (s)	5000	5000	5000	5000
Velocity (m/s)	0.27	0.28	0.3	0.36
Wall Friction	0.5	0.5	0.5	0.5
Particle Surface Adhesion	0	0	0	0
Stress Precision Index	1	1	1	1
Tessellation Tolerance	3	3	3	3

Table E-4 Feeders for Delayed Configuration

Component Name	Feeder_FS/NS_S0	Feeder_FS/NS_S20_Del	Feeder_FS/NS_S23_Del	Feeder_FS/NS_S28_Del	Feeder_FS/NS_S30_Del
Time on (s)	-1	3.9/13.9	3.9/13.9	3.9/13.9	3.9/13.9
Time off (s)	4/14	5000	5000	5000	5000
Velocity (m/s)	0	0.2	0.23	0.28	0.3
Wall Friction	0.5	0.5	0.5	0.5	0.5
Particle Surface Adhesion	0	0	0	0	0
Stress Precision Index	1	1	1	1	1
Tessellation Tolerance	3	3	3	3	3

Table E-5 Chutes

Component Name	Chute_Skirts	Chute_Feeder	Chute_Hopper	Chute_Skirts-3	Chute_Feeder-3	Chute_Hopper-3
Time on (s)	-1	-1	-1	-1	-1	-1
Time off (s)	5000	5000	5000	5000	5000	5000
Wall Friction	0.5	0.5	0.5	0.3	0.3	0.3
Particle Surface Adhesion	0	0	0	0	0	0
Stress Precission Index	1	1	1	1	1	1
Tessellation Tolerance	3	3	3	3	3	3

Table E-6 Material Radius 15 mm to 20 mm

Material Name	Ore_SS15_R	Ore_SS20_R	Ore_C22_1_R	Ore_C22_2_R	Ore_D22_S	Ore_D22_R	Ore_D22_I
Bulk Density (kg/m^3)	1900	1900	1900	1900	1900	1900	1900
Packing Ratio	1.5	1.5	1.5	1.5	1.5	1.5	1.5
Particle Density (kg/m^3)	2850	2850	2850	2850	2850	2850	2850
Conditions	Rough	Rough	Rough	Rough	Smooth	Rough	Interlocking
Interparticle Friction	0.3	0.3	0.3	0.3	0.2	0.3	0.6
Particle Size Distribution	Random	Random	Random	Random	Random	Random	Random
Max Radius (mm)	15	20	22	22	22	22	22
Min Radius (mm)	12	18	20	20	20	20	20
Cohesive Condition	Slightly Sticky	Slightly Sticky	Custom	Custom	Dry	Dry	Dry
Interparticle Cohesion	0.7564	0.6389	0.2	0.01	0	0	0
Radius of Fines	0.5895	0.6519	0.6781	0.6781	0	0	0

Table E-7 Material radius 40 mm

Material Name	Ore_SS40_R	Ore_SS40_R	Ore_D40_S	Ore_D40_R	Ore_C40_1_S	Ore_C40_2_R
Bulk Density (kg/m^3)	1900	1900	1900	1900	1900	1900
Packing Ratio	1.5	1.5	1.5	1.5	1.5	1.5
Particle Density (kg/m^3)	2850	2850	2850	2850	2850	2850
Conditions	Rough	Rough	Smooth	Rough	Smooth	Rough
Interparticle Friction	0.3	0.3	0.2	0.3	0.2	0.3
Particle Size Distribution	Random	Random	Random	Random	Random	Random
Max Radius (mm)	40	40	40	40	40	40
Min Radius (mm)	40	40	40	40	40	40
Cohesive Condition	Slightly Sticky	Slightly Sticky	Dry	Dry	Custom	Custom
Interparticle Cohesion	0.1596	0.1596	0	0	0	0
Radius of Fines	0.9547	0.9547	0	0	0.9547	0.9547

Table E-8 Simulation Basic Configuration

Simulation Name	**Chute Friction**	**Hopper Height**	**Injection Box**	**Belt**	**Feeder**	**Material**	**Simulation Time (s)**
FP_Original_1	0.5	500	Inj_FS_1300	RC01_Fr32_S30	Feeder_FS/NS_S27	Ore_SS40_R	20
FP_Original_2	0.5	500	Inj_FS_1300	RC01_Fr50_S216	Feeder_FS/NS_S37	Ore_SS40_R	25
FP_Original_3	0.5	500	Inj_FS_1300	RC01_Fr32_S30	Feeder_FS/NS_S27	Ore_SS15_R	20
FP_Original_4	0.5	500	Inj_FS_1300	RC01_Fr50_S30	Feeder_FS/NS_S28	Ore_SS20_R	25
FP_Original_5	0.5	500	Inj_FS_1300	RC01_Fr50_S216	Feeder_FS/NS_S37	Ore_D22_R	25
FP_Original_9	0.5	500	Inj_FS_1300	RC01_Fr50_S216	Feeder_FS/NS_S37	Ore_D40_R	25
FP_Original_12	0.5	500	Inj_FS_1150	RC01_Fr50_S216	Feeder_FS/NS_S36	Ore_D22_I	13.1
FP_Original_13	0.5	500	Inj_FS_1150	RC01_Fr50_S216	Feeder_FS/NS_S36	Ore_C22_1_R	25
FP_Original_14	0.5	500	Inj_FS_1150	RC01_Fr50_S216	Feeder_FS/NS_S36	Ore_D40_R	25
FP_Original_15	0.5	500	Inj_FS_1150	RC01_Fr50_S216	Feeder_FS/NS_S30	Ore_D40_S	25
FP_Original_16	0.5	500	Inj_FS_1150	RC01_Fr50_S216	Feeder_FS/NS_S28	Ore_D40_S	25
FP_Original_17	0.5	500	Inj_FS_1150	RC01_Fr50_S216	Feeder_FS/NS_S28	Ore_D22_S	25

Table E-9 Simulation Basic Results

Simulation Name	**Time to run (min)**	**Particles**	**Mass Balance**	**Material Spread**	**Slumping**	**Comments**
FP_Original_1	49.2395	11,980	No	Poor	Marginal	Feeder slow, conveyor fast, material role back
FP_Original_2	34.3797	9,102	Yes	Poor	Good	Material too sticky
FP_Original_3	827.2096	248,123	No	Poor	Marginal	Feeder slow, conveyor fast, material role back, simulation stopped at 12.1997 as exceeded 250,000 particles.
FP_Original_4	539.2648	103,508	No	Poor	Good	Feeder slow, conveyor fast, material clumping heavily
FP_Original_5	276.121	54,707	No	Good	Poor	Feeder fast
FP_Original_7	33.1971	8,920	No	Good	Poor	Feeder slightly fast
FP_Original_8	91.5262	53,594	Yes	Poor	Good	Material too sticky
FP_Original_9	281.0227	54,157	No	Poor	Poor	Feeder fast, Material too sticky
FP_Original_10	25.4551	7,911	No	Good	Marginal	Feeder fast
FP_Original_11	30.2475	8,954	No	Good	Poor	Feeder Fast
FP_Original_12	30.6218	9,392	Yes	Good	Poor	Good Simulation
FP_Original_13	282.965	63,211	Yes	Good	Poor	Good Simulation

Table E-10 Simulation Delay Start Configuration

Simulation Name	**Chute Friction**	**Hopper Height**	**Injection Box**	**Belt**	**Feeder**	**Feeder**	**Material**	**Simulation Time (s)**
FP_Original_18	0.5	500	Inj_FS_1150_Del	RC01_Fr50_S216	Feeder_FS/NS_S0	Feeder_FS/NS_S28_Del	Ore_D40_S	40
FP_Original_19	0.5	500	Inj_FS_1150_Del	RC01_Fr50_S216	Feeder_FS/NS_S0	Feeder_FS/NS_S28_Del	Ore_D22_S	40
FP_Original_20	0.5	500	Inj_FS_1150_Del	RC01_Fr50_S216	Feeder_FS/NS_S0	Feeder_FS/NS_S30_Del	Ore_D22_R	40
FP_Original_21	0.3	700	Inj_FS_1150_Del	RC01_Fr50_S216	Feeder_FS/NS_S0	Feeder_FS/NS_S20_Del	Ore_D40_S	40
FP_Original_22	0.3	700	Inj_FS_1150_Del	RC01_Fr50_S216	Feeder_FS/NS_S0	Feeder_FS/NS_S30_Del	Ore_D40_R	40
FP_Original_23	0.3	700	Inj_FS_1150_Del	RC01_Fr50_S216	Feeder_FS/NS_S0	Feeder_FS/NS_S28_Del	Ore_C40_2_R	40
FP_Original_24	0.3	700	Inj_FS_1150_Del	RC01_Fr50_S216	Feeder_FS/NS_S0	Feeder_FS/NS_S30_Del	Ore_C40_1_S	40
FP_Original_25	0.3	700	Inj_FS_1150_Del	RC01_Fr50_S216	Feeder_FS/NS_S0	Feeder_FS/NS_S20_Del	Ore_D22_S	40
FP_Original_26	0.3	700	Inj_FS_1150_Del	RC01_Fr50_S216	Feeder_FS/NS_S0	Feeder_FS/NS_S30_Del	Ore_C22_2_R	40
FP_Original_28	0.3	700	Inj_FS_1150_Del	RC01_Fr50_S216	Feeder_FS/NS_S0	Feeder_FS/NS_S20_Del	Ore_D22_R	40
FP_Original_29	0.3	600	Inj_FS_1150_Del	RC01_Fr50_S216	Feeder_FS/NS_S0	Feeder_FS/NS_S23_Del	Ore_D40_S	40
FP_Original_30	0.3	600	Inj_FS_1150_Del	RC01_Fr50_S216	Feeder_FS/NS_S0	Feeder_FS/NS_S24_Del	Ore_D40_R	40
FP_Original_31	0.3	600	Inj_FS_1150_Del	RC01_Fr50_S216	Feeder_FS/NS_S0	Feeder_FS/NS_S23_Del	Ore_D22_S	40
FP_Original_32	0.3	600	Inj_FS_1150_Del	RC01_Fr50_S216	Feeder_FS/NS_S0	Feeder_FS/NS_S23_Del	Ore_D22_R	40

Table E-11 Simulation Delay Start Results

Simulation Name	**Time to run (min)**	**Particles**	**Mass Balance**	**Material Spread**	**Slumping**	**Comments**
FP_Original_18	59.691	11243	No	Good	Marginal	Feeder slow. Good material Spread
FP_Original_19	494.571	72314	No	Good	Poor	Feeder slow. Very good material spread. No slumping seen.
FP_Original_20	514.2934	70365	Yes	Good	Marginal	Good material. Some minor surging, No slumping seen.
FP_Original_21	66.7516	12020	Yes	Good	Marginal	Minor surging on single feed. Some material spread
FP_Original_22	70.4611	12843	Yes	Marginal	Good	Surging seen on single feeder. No material spread.
FP_Original_23	58.8883	12888	Yes	Marginal	Marginal	Minor surging on single feed. Some material spread
FP_Original_24	59.4384	12016	No	Good	Marginal	Feeder slow. Some surging. Good spread
FP_Original_25	542.75	77881	Yes	Good	Marginal	Excellent spread, little to no surging
FP_Original_26	637.8705	87390	No	Marginal	Marginal	Some surging and some spread.
FP_Original_28	567.3739	-	No	Good	Marginal	Feeder Slow, excellent spread, little to no surging
FP_Original_29	57.7114	10483	Yes	Good	Marginal	Excellent spread, little to no surging
FP_Original_30	90.9373	11854	Yes	Good	Marginal	Excellent spread, little to no surging
FP_Original_31	405.6016	73366	Yes	Good	Marginal	Excellent spread, little to no surging
FP_Original_32	561.324	84520	Yes	Good	Marginal	Excellent spread, little to no surging

Table E-12 Feeder Extensions

Component Name	Feeder_FS/NS_S23_ext	Feeder_FS/NS_S30_ext	Feeder_FS/NS_S30_ext2
Time on (s)	3.9/13.9	3.9/13.9	3.9/13.9
Time off (s)	5000	5000	5000
Velocity (m/s)	0.23	0.3	0.3
Wall Friction	0.5	0.5	0.5
Particle Surface Adhesion	0	0	0
Stress Precision Index	1	1	1
Tessellation Tolerance	3	3	3

Table E-13Inserts

Component Name	Insert_1	Insert_2	Insert_3
Time on (s)	-1	-1	-1
Time off (s)	5000	5000	5000
Wall Friction	0.5	0.5	0.5
Particle Surface Adhesion	0	0	0
Stress Precission Index	1	1	1
Tessellation Tolerance	3	3	3

The following components and parameters are common to tables Table E-14, Table E-15 and Table E-16:

- Belt: RC01_Fr50_S216
- Maximum Velocity: 9.5 m/s
- Injection Box: Inj_FS_1150

Table E-14 Simulation Configuration & Results for Insert Only

Simulation Name	**Chute Friction**	**Hopper Height**	**Insert**	**Feeder**	**Material**	**Simulation Time (s)**	**Run Time (min)**	**Mass Balance**	**Comments**
FP_ Insert_1	0.5	500	Insert_1	Feeder_FS/NS_S28	Ore_D40_S	40	31.4742	Yes	Chute Blocked
FP_ Insert_2	0.5	500	Insert_1	Feeder_FS/NS_S28	Ore_D40_R	13.2978	12.963	Yes	Chute Blocked
FP_ Insert_3	0.5	500	Insert_2	Feeder_FS/NS_S28	Ore_D40_S	40	63.8292	Yes	Chute Blocked

Table E-15 Simulation Configuration & Results for Feeder Extension Only

Simulation Name	**Chute Friction**	**Hopper Height**	**Feeder / Extension**	**Material**	**Simulation Time (s)**	**Run Time (min)**	**Mass Balance**	**Comments**
FP_Orig_Ext_1	0.5	500	Feeder_FS/NS_S28_Del* / Feeder_FS/NS_S28_Ext	Ore_D40_S	40	69.2952	Yes	Material loaded centrally, some profile development
FP_Orig_Ext_2	0.5	500	Feeder_FS/NS_S28_Del* / Feeder_FS/NS_S28_Ext	Ore_D22_S	40	500.1894	No	Material loaded centrally Feeder slightly slow, some profile development
FP_Orig_Ext_3	0.5	500	Feeder_FS/NS_S30_Del* / Feeder_FS/NS_S30_Ext	Ore_D22_R	40	505.0964	Yes	Material loaded centrally, some profile development
FP_Orig_Ext_8	0.3	600	Feeder_FS/NS_S23_Del* / Feeder_FS/NS_S23_Ext	Ore_D22_S	40	535.4561	Yes	Material loaded centrally, some profile development
FP_Orig_Ext_9	0.3	600	Feeder_FS/NS_S23_Del* / Feeder_FS/NS_S23_Ext	Ore_D22_R	40	581.9149	Yes	Material loaded centrally, some profile development

* Includes Feeder_FS/NS_S0

Table E-16 Simulation Configuration & Results for Feeder Extension & Insert

	Chute Friction	**Insert**	**Feeder**	**Material**	**Simulation Time (s)**	**Run Time (min)**	**Mass Balance**	**Comments**
FP_Orig_Ext_4	0.5	Insert_3	Feeder_FS/NS_S30_Del*	Ore_D40_R	40	66.0793	No	Good Profile formation, central feed, feeder slightly slow.
FP_Orig_Ext_5	0.5	Insert_3	Feeder_FS/NS_S30_Del*	Ore_D40_S	40	57.7883	No	Good Profile formation, central feed, feeder slightly slow.
FP_Orig_Ext_6	0.5	Insert_3	Feeder_FS/NS_S30_Del*	Ore_D22_R	40	209.5943	Yes	Good Profile formation, central feed, Simulation stopped at 21.9 s.
FP_Orig_Ext_7	0.5	Insert_3	Feeder_FS/NS_S30_Del*	Ore_D22_S	40	513.5587	Yes	Good Profile formation, central feed.
FP_Orig_Ext_10	0.3	Insert_3	Feeder_FS/NS_S23_Del*	Ore_D22_R	40	-	Yes	Good Profile formation, central feed.
FP_Orig_Ext_11	0.3	Insert_3	Feeder_FS/NS_S23_Del*	Ore_D22_S	40	-	Yes	Good Profile formation, central feed.

* Includes Feeder_FS/NS_S0